Bayesian Inference for Improved Single Molecule Fluorescence Tracking

Ji Won Yoon,*† Andreas Bruckbauer,† William J. Fitzgerald,* and David Klenerman†
*Department of Engineering and †Department of Chemistry, University of Cambridge, Cambridge, United Kingdom

ABSTRACT Single molecule tracking is widely used to monitor the change in position of lipids and proteins in living cells. In many experiments in which molecules are tagged with a single or small number of fluorophores, the signal/noise ratio may be limiting, the number of molecules is not known, and fluorophore blinking and photobleaching can occur. All these factors make accurate tracking over long trajectories difficult and hence there is still a pressing need to develop better algorithms to extract the maximum information from a sequence of fluorescence images. We describe here a Bayesian-based inference approach, based on a trans-dimensional sequential Monte Carlo method that utilizes both the spatial and temporal information present in the image sequences. We show, using model data, where the real trajectory of the molecule is known, that our method allows accurate tracking of molecules over long trajectories even with low signal/noise ratio and in the presence of fluorescence blinking and photobleaching. The method is then applied to real experimental data.

INTRODUCTION

Using fluorescence microscopy with single-molecule sensitivity, it is now possible to follow to movement of individual fluorophore tagged molecules such as proteins and lipids in the cell membrane with nanometer precision (1–3). Using single molecule tracking, diffusion or directed motion of molecules on the cell can be investigated to elucidate the structure of the cell membrane. To date, most methods have been based on nonlinear least-square fitting of the fluorescence images to Gaussian functions and while automated tracking algorithms exist, quite often manual input is necessary (4,5). The number of molecules has to be known and most software cannot handle the appearance of additional objects during tracking. This frequently happens when the density of molecules is high at the beginning of the image sequence so that they are initially so close together that they cannot be resolved separately and later move apart (6). Another problem is that due to low signal/noise ratio, some molecules cannot be detected in individual frames so that longer tracks are split into shorter sections. Long trajectories are usually needed to get good statistics for diffusion analysis whereas the typical observation time of the fluorophore, before irreversible photobleaching occurs, sets a limit to the length of trajectories. Furthermore deterministic methods, where no randomness is assumed, detect spots with regional maxima (7). They usually require us to set a threshold and the detection is very sensitive to this threshold setting. For experimental data, the correct threshold is usually not known. To be computationally efficient, a well-known deterministic method selects the threshold at the upper 30th percentile of brightness for the entire image (8). However, the threshold-based method may fail to detect real spots which are less bright than the threshold. Also, most algorithms for single molecule tracking focus only on fitting of spatial information (9–11). Since we are processing a set of sequential images, we have used both temporal and spatial information. Specifically we have used a Bayesian-based approach, which uses prior information in time and space about the molecule trajectory and does not require a strict threshold.

The tracking of single dye-conjugated molecules is a multitarget tracking problem with each target a fluorescent signal. We have developed a sequential Monte Carlo (SMC) algorithm which considers spatial and temporal information of the molecular motion since this gives longer and more accurate tracks. The SMC algorithm can also track several molecules simultaneously. However, the number of molecules is not known, a priori, since the number of targets may be different in each frame. To cope with the unknown number of targets, we have used trans-dimensional SMC where the number of dimensions can change with time. We also require parameter association for this trans-dimensional SMC method to identify the correct molecules in each frame. In this article, we solve the parameter association problem by clustering parameters using expectation maximization (EM) algorithm. Each target for tracking via our SMC method is represented by a Gaussian profile with unknown center coordinate, amplitude, and width (12–14). The proposed algorithm based on the track-before-detection (TBD) scheme uses original data (15,16). Therefore, we can avoid the information loss which may happen in the threshold-based detection algorithm (8,17). In case of low signal/noise ratio (SNR), our modified SMC algorithm with TBD scheme may detect weak signals.

The remainder of the article is organized as follows. The Theory section gives the philosophy of the Bayesian inference as used in this article. The Sequential Monte Carlo (SMC) section introduces the Bayesian sequential estimation framework, which leads to a particular trans-dimensional SMC approach. The Fluorescence Image section discusses the modeling assumptions such as prior information for the single molecule fluorescence images. The main algorithms for the

Submitted June 27, 2007, and accepted for publication February 8, 2008.

Address reprint requests to David Klenerman, Tel.: 44-1-22-333-6481; E-mail: dk10012@cam.ac.uk.

Editor: Michael Edidin.

0006-3495/08/06/4932/16 $2.00

doi: 10.1529/biophysj.107.116285

Estimation of the Source-by-Source Effect of Autorepression on Genetic Noise

Hiroyuki Okano,* Tetsuya J. Kobayashi,†‡ Hirokazu Tozaki,§ and Hidenori Kimura*
*Bio-Mimetic Control Research Center, The Institute of Physical and Chemical Research, RIKEN, Nagoya, Japan; †Research Fellow of the Japan Society for the Promotion of Science, ‡Center for Developmental Biology, The Institute of Physical and Chemical Research, RIKEN, Kobe, Japan; and §ERATO Aihara Complexity Modeling Project, JST, Tokyo, Japan

ABSTRACT Transcriptional autorepression has been thought to be one of the simplest control circuits to attenuate fluctuations in gene expression. Here, we explored the effect of autorepression on fluctuations from different noise sources. We theoretically represent the fluctuations in the copy number of proteins as the sum of several terms, each of which is related to a specific noise source and expressed as the product of the source-specific fluctuations under no autorepression (path gain) and the effect of autorepression on them (loop gain). Inspection of each term demonstrates the source-independent noise-attenuating effect of autorepression as well as its source-dependent efficiency. Our experiments using a synthetic autorepression module revealed that autorepression attenuates fluctuations of various noise compositions. These findings indicate that the noise-attenuating effect of autorepression is robust against variation in noise compositions. We also experimentally estimated the loop gain for mRNA noise, demonstrating that loop gains are measurable parameters. Decomposition of fluctuations followed by experimental estimation of path and loop gains would help us to understand the noise-related feature of design principles underlying loop-containing biological networks.

INTRODUCTION

Biochemical reactions are inherently stochastic. Low abundance of some key cellular components, including DNA, mRNA, and some regulatory proteins, makes such the stochastic nature of biochemical reactions prominent, leading to large concentration fluctuations of reaction products (1–7). Because cellular functions must be executed through biochemical networks whose components are potentially noisy, cells must have evolved network architectures for efficient attenuation or utilization of noise (8–10).

Progression of biochemical reactions is under elaborate control by cellular machineries that by themselves result from biochemical reactions. Production of cellular components therefore involves a number of biochemical reactions, and consequently, a number of potential noise sources. Hence, fluctuations in the copy number of cellular components would originate from various noise sources, and the composition of fluctuations would be different from one cellular component to another. A recent study showed that both global and specific noise sources contribute to total fluctuations (11). Because such difference in a noise composition should influence the efficiency of noise attenuation by a specific control architecture, noise composition is a crucial factor for the cellular design of noise-control networks.

Noise compositions have been extensively studied for open-loop gene circuits both theoretically and experimentally (2,3,12,13). Because intracellular networks contain many loop structures, it is challenging to explore contributions from individual noise sources in loop-containing networks. In this study, we focused on a transcriptional autorepression circuit as the simplest loop-containing cellular circuit.

Transcriptional autorepression accounts for ~90% of transcriptional feedback loops in *Escherichia coli* (14). Despite its simplicity, the autorepression circuit is composed of several reactions, and thus involves several potential noise sources. The effect of autorepression on total fluctuations has been extensively studied both experimentally (15,16) and theoretically (12,17,18). There have been few studies, however, on the effect of autorepression in terms of noise composition. For instance, the previous experiments measured fluctuations in gene expression on plasmids where fluctuations in plasmid copy numbers would be dominant (15,16, 19). It is therefore still uncertain whether autorepression could act in the same manner on fluctuations of a different noise composition, such as those in chromosomal gene expression. It is also of physiological interest to examine how autorepression affects fluctuations in chromosomal gene expression in the light of its frequent appearance in *E. coli*.

For theory, Simpson and his colleagues reported a formal expression in a frequency domain for the effect of autorepression on fluctuations derived from any noise source

Submitted October 30, 2007, and accepted for publication March 18, 2008.

Hiroyuki Okano and Tetsuya J. Kobayashi contributed equally to this work. Hiroyuki Okano conducted all experimental works, and Tetsuya J. Kobayashi constructed the basic theory of the source-by-source contribution and efficiency of autorepression, and that of error estimation due to model simplification. Both of them contributed to constructing the strategy to experimentally measure the mRNA loop gain and theoretically proving the order of the efficiencies of loop gains.

Address reprint requests to H. Okano, Tel.: 81-52-736-5861; E-mail: okano@bmc.riken.jp.

Editor: Arthur Sherman.

0006-3495/08/08/1063/12 $2.00

doi: 10.1529/biophysj.107.124677

Tightly Regulated and Heritable Division Control in Single Bacterial Cells

Dan Siegal-Gaskins* and Sean Crosson†
*Department of Physics and †Department of Biochemistry and Molecular Biology, and The Committee on Microbiology, University of Chicago, Chicago, Illinois 60637

ABSTRACT The robust surface adherence property of the aquatic bacterium *Caulobacter crescentus* permits visualization of single cells in a linear microfluidic culture chamber over an extended number of generations. The division rate of *Caulobacter* in this continuous-flow culture environment is substantially faster than in other culture apparati and is independent of flow velocity. Analysis of the growth and division of single isogenic cells reveals that the cell cycle control network of this bacterium generates an oscillatory output with a coefficient of variation lower than that of all other bacterial species measured to date. DivJ, a regulator of polar cell development, is necessary for maintaining low variance in interdivision timing, as transposon disruption of *divJ* significantly increases the coefficient of variation of both interdivision time and the rate of cell elongation. Moreover, interdivision time and cell division arrest are significantly correlated between mother and daughter cells, providing evidence for epigenetic inheritance of cell division behavior in *Caulobacter*. The single-cell growth/division results reported here suggest that future predictive models of *Caulobacter* cell cycle regulation should include parameters describing the variance and inheritance properties of this system.

INTRODUCTION

Studies of single microbial cells have revealed remarkable variability in the level of individual gene expression, rate of cell growth, and timing of cell division (1–3). Microfluidic devices have recently emerged as tools for studying dynamic processes at the single-cell level (4–6), with a number of studies reporting the use of microfluidics in quantifying single-cell growth and division (7–9). Such studies of single-cell behavior have been extremely valuable, yielding insights into phenomena that are not revealed in population-wide measurements (10–14). Although experiments that image single cells over short timescales on either agarose/gelatin pads or in microfluidic devices have become relatively routine, long-term and multigenerational studies of single cells have been complicated by problems with perturbative cell immobilization protocols or by rapid accumulation of cells on the pad or inside the microfluidic device.

The freshwater α-proteobacterium *Caulobacter crescentus* (15) (henceforth referred to as *Caulobacter*) naturally allows for experiments that do not suffer from the aforementioned problems and is thus an ideal model to probe single-cell behavior across multiple generations (16). *Caulobacter* exists in two unique states during its cell cycle: a "swarmer" (SW) state, in which the cell possesses polar type IV pili and a single polar flagellum, and a nonmotile "stalked" (ST) state (Fig. 1). Differentiation from SW to ST occurs just before the initiation of DNA replication, at which time the flagellum is released, the pili are retracted, and a narrow cylindrical extension of the cell envelope known as the stalk is grown in their place. At the tip of the stalk is a structure known as the holdfast, which contains an exceptionally strong polysaccharide adhesive (17,18). Toward the end of the ST stage, a new flagellar assembly and pili are constructed at the pole opposite the stalk, and on division, a new motile, chemotactic SW cell is spawned. The SW cell then progresses through the full cell cycle, whereas the adhesive ST cell commences another round of DNA replication and division.

The natural adhesive properties of *Caulobacter* allowed us to conduct a multigenerational single-cell study of growth and division in a linear microfluidic culture chamber under temporally homogeneous and minimally perturbative conditions. We show that division of *Caulobacter* ST cells under constant medium flow is rapid and tightly regulated (i.e., exhibits low variance) relative to other bacterial species. Disruption of the gene encoding the DivJ histidine kinase, a core regulator of polar cell development (19,20), significantly increases variance in interdivision timing relative to the mean interdivision time. In addition, we show that factors controlling generational timing and division arrest are inherited from mother ST cells to daughter SW cells epigenetically, resulting in correlated cell division behavior between mother and daughter cells in the same generational window. This intragenerational correlation suggests that the network controlling *Caulobacter* cell division has determinsitic properties in which the current state of a cell influences future divisions.

Submitted January 7, 2008, and accepted for publication April 18, 2008.

Address reprint requests to Sean Crosson, Dept. of Biochemistry and Molecular Biology, University of Chicago, 929 E. 57th St., W125, Chicago, IL 60637. Tel.: 773-834-1926; Fax: 773-702-0439; E-mail: scrosson@uchicago.edu.

Editor: Alexander Mogilner.

0006-3495/08/08/2063/10 $2.00

METHODS

Microfluidic growth and division assays

Microfluidic channels measuring 200 μm wide by 50 μm deep by 2 cm long were made with polydimethylsiloxane (PDMS, Sylgard Brand 184 Silicone

doi: 10.1529/biophysj.108.128785

formy stalk, using for visualization
study cell adhesion cell elongation rate very constant

The EMBO Journal (2008) 27, 2725–2735 | © 2008 European Molecular Biology Organization | All Rights Reserved 0261-4189/08
www.embojournal.org

THE EMBO JOURNAL

Curing of the [URE3] prion by Btn2p, a Batten disease-related protein

Dmitry S Kryndushkin, Frank Shewmaker and Reed B Wickner*

Laboratory of Biochemistry and Genetics, National Institute of Diabetes and Digestive and Kidney Diseases, National Institutes of Health, Bethesda, MD, USA

[URE3] is a prion (infectious protein), a self-propagating amyloid form of Ure2p, a regulator of yeast nitrogen catabolism. We find that overproduction of Btn2p, or its homologue Ypr158 (Cur1p), cures [URE3]. Btn2p is reported to be associated with late endosomes and to affect sorting of several proteins. We find that double deletion of *BTN2* and *CUR1* stabilizes [URE3] against curing by several agents, produces a remarkable increase in the proportion of strong [URE3] variants arising *de novo* and an increase in the number of [URE3] prion seeds. Thus, normal levels of Btn2p and Cur1p affect prion generation and propagation. Btn2p–green fluorescent protein (GFP) fusion proteins appear as a single dot located close to the nucleus and the vacuole. During the curing process, those cells having both Ure2p–GFP aggregates and Btn2p–RFP dots display striking colocalization. Btn2p curing requires cell division, and our results suggest that Btn2p is part of a system, reminiscent of the mammalian aggresome, that collects aggregates preventing their efficient distribution to progeny cells.

The EMBO Journal (2008) **27**, 2725–2735. doi:10.1038/emboj.2008.198; Published online 2 October 2008
Subject Categories: membranes & transport; proteins
Keywords: amyloid; Hook homologue; Ypr158p

Introduction

The infectious proteins (prions) of yeast, [URE3] and [*PSI*$^+$], are self-propagating amyloid forms of Ure2p and Sup35p, respectively (Wickner, 1994; King and Diaz-Avalos, 2004; Tanaka *et al*, 2004; Brachmann *et al*, 2005). Both amyloids are parallel in-register β-sheet structures (Shewmaker *et al*, 2006; Baxa *et al*, 2007).

The generation and propagation of these amyloids are critically affected by many chaperones and their auxiliary factors. The disaggregating chaperone Hsp104 is necessary for both prions, and its overproduction leads to the loss of [*PSI*$^+$] (Chernoff *et al*, 1995; Moriyama *et al*, 2000). The soluble cytoplasmic Hsp70s (Ssa proteins) affect the propagation of both prions (Jung *et al*, 2000; Roberts *et al*, 2004) and protect [*PSI*$^+$] from curing by overproduction of Hsp104 (Newnam *et al*, 1999). Overexpression of Hsp40s destabilizes both [URE3] (Moriyama *et al*, 2000) and in some cases [*PSI*$^+$] (Kushnirov *et al*, 2000). Hsp104, in cooperation with Hsp70s and Hsp40s disaggregate proteins (Glover and Lindquist, 1998), and these chaperones apparently function together to break long amyloid filaments into shorter ones, thereby creating new 'seeds' to propagate the prions (Kushnirov and Ter-Avanesyan, 1998). Among other chaperones affecting [*PSI*$^+$] propagation are the ribosome-associated Hsp70s, called Ssb's (Chernoff *et al*, 1999); several co-chaperones of Hsp70s, such as Sti1p and Cpr7p (Jones *et al*, 2004) and the nucleotide exchange factors for Hsp70s, Fes1p and Sse1p (Jones *et al*, 2004; Fan *et al*, 2007; Kryndushkin and Wickner, 2007). The effects of many of these factors on Hsp70s, and mutations of Hsp70s, indicate that the stabilization of the ATP-bound form of Ssa1p promotes [*PSI*$^+$] propagation, whereas the ADP-bound form destabilizes [*PSI*$^+$] (Jones *et al*, 2004). For [URE3], the alteration of Ssa1 activity in either direction can damage prion propagation (Kryndushkin and Wickner, 2007), suggesting that the normal level of Hsp70 activity is required for [URE3].

Other factors affecting prion propagation in yeast include cytoskeletal proteins (Ganusova *et al*, 2006) and elements of the ubiquitin system (Allen *et al*, 2007). In addition, [*PSI*$^+$], and to a lesser extent [URE3], prion generation is promoted by another prion called [*PIN*$^+$] (for Psi inducibility), which is an amyloid of the Rnq1 protein (Derkatch *et al*, 2001; Bradley *et al*, 2002).

Here, we identify Btn2p and its homologue, Ypr158p (Cur1p) as proteins able to destabilize [URE3]. We find that Btn2p curing of [URE3] involves colocalization of Ure2p prion aggregates and the Btn2 protein. Moreover, normal levels of Btn2p and Cur1p lower [URE3] prion seeds and affect the spectrum of prion variants arising.

Results

Identification of Btn2p and Ypr158p (Cur1p) as factors that can destabilize [URE3]

We recently described a genomic screen for prion-eliminating factors (Kryndushkin and Wickner, 2007). Strain BY241, bearing *ADE2* under control of the *DAL5* promoter (Brachmann *et al*, 2005), was used to monitor the activity of Ure2p. Prion inactivation of Ure2p allows *ADE2* transcription, resulting in pink or white colonies according to the level of transcription, whereas active Ure2p makes such a strain Ade− and red on adenine-limiting medium. Utilizing this system, we showed that overproducing the chaperones Ydj1p and Sse1p could cure [URE3] (Kryndushkin and Wickner, 2007). Here, we show that overproduced Btn2p and Ypr158p (which we name Cur1p for 'Curing of [URE3]') are also prion-curing factors. Overexpression of either *BTN2* or *CUR1* in the strain BY241 [URE3] v1 (a mitotically stable [URE3] prion

*Corresponding author. Laboratory of Biochemistry and Genetics, National Institute of Diabetes and Digestive and Kidney Diseases, National Institutes of Health, Building 8, Room 225, 8 Center Drive, MSC0830, Bethesda, MD 20892-0830, USA. Tel.: +1 301 496 3452; Fax: +1 301 402 0240; E-mail: wickner@helix.nih.gov

Received: 22 May 2008; accepted: 9 September 2008; published online: 2 October 2008

A Publication of The Genetics Society of America

GENETICS

Originally published as *Genetics* Published Articles Ahead of Print on August 30, 2008.

Genetics, Vol. 180, 431-443, September 2008, Copyright © 2008
doi:10.1534/genetics.108.091330

Genetic Basis of Evolutionary Adaptation by *Escherichia coli* to Stressful Cycles of Freezing, Thawing and Growth

Sean C. Sleight[*,1], Christian Orlic[*], Dominique Schneider[†,‡] and Richard E. Lenski[*]

[*] Department of Microbiology and Molecular Genetics, Michigan State University, East Lansing, Michigan 48824, [†] Laboratoire Adaptation et Pathogénie des Micro-organismes, Université Joseph Fourier Grenoble 1, F-38042 Grenoble Cedex 9, France and [‡] CNRS UMR 5163, F-38042 Grenoble Cedex 9, France

[1] *Corresponding author:* Department of Bioengineering, University of Washington, Seattle, WA 98195.
E-mail: sleight@u.washington.edu

Microbial evolution experiments offer a powerful approach for coupling changes in complex phenotypes, including fitness and its components, with specific mutations. Here we investigate mutations substituted in 15 lines of *Escherichia coli* that evolved for 1000 generations under freeze–thaw–growth (FTG) conditions. To investigate the genetic basis of their improvements, we screened many of the lines for mutations involving insertion sequence (IS) elements and identified two genes where multiple lines had similar mutations. Three lines had IS*150* insertions in *cls*, which encodes cardiolipin synthase, and 8 lines had IS*150* insertions in the *uspA-uspB* intergenic region, encoding two universal stress proteins. Another line had an 11-bp deletion mutation in the *cls* gene. Strain reconstructions and competitions demonstrated that this deletion is beneficial under the FTG regime in its evolved genetic background. Further experiments showed that this *cls* mutation helps maintain membrane fluidity after freezing and thawing and improves freeze–thaw (FT) survival. Reconstruction of isogenic strains also showed that the IS*150* insertions in *uspA/B* are beneficial under the FTG regime. The evolved insertions reduce *uspB* transcription and increase both FT survival and recovery, but the physiological mechanism for this fitness improvement remains unknown.

THIS ARTICLE
Full Text
Full Text (PDF)
Data Supplement
All Versions of this Article:
genetics.108.091330v1
180/1/431 *most recent*
Alert me when this article is cited
Alert me if a correction is posted

SERVICES
Related articles in Genetics
Similar articles in this journal
Similar articles in PubMed
Alert me to new issues of the journal
Download to citation manager
Reprints & Permissions

GOOGLE SCHOLAR
Articles by Sleight, S. C.
Articles by Lenski, R. E.

PUBMED
PubMed Citation
Articles by Sleight, S. C.
Articles by Lenski, R. E.

Related articles in Genetics:

ISSUE HIGHLIGHTS

Genetics 2008 180: NP. **[Full Text]**

Online ISS 1091-6490

phone: 412-268-1812 fax: 412-268-1813 email: genetics-gsa@andrew.cmu.edu

J|A|C|S
ARTICLES
Published on Web 09/20/2008

Highly Stable Organic Monolayers for Reacting Silicon with Further Functionalities: The Effect of the C−C Bond nearest the Silicon Surface

Sreenivasa Reddy Puniredd, Ossama Assad, and Hossam Haick*

The Department of Chemical Engineering and Russell Berrie Nanotechnology Institute, Technion—Israel Institute of Technology, Haifa 32000, Israel

Received June 19, 2008; E-mail: hhossam@technion.ac.il

Abstract: Crystalline Si(111) surfaces have been alkylated in a two-step chlorination/alkylation process using various organic molecules having similar backbones but differing in their C−C bond closest to the silicon surface (i.e., C−C vs C=C vs C≡C bonds). X-ray photoelectron spectroscopic (XPS) data show that functionalization of silicon surfaces with propenyl magnesium bromide (CH_3−CH=CH−MgBr) organic molecules gives nearly full coverage of the silicon atop sites, as on methyl- and propynyl-terminated silicon surfaces. Propenyl-terminated silicon surface shows less surface oxidation and is more robust against solvent attacks when compared to methyl- and propynyl-terminated silicon surfaces. We also show a secondary functionalization process of propenyl-terminated silicon surface with 4′-[3-Trifluoromethyl-3H-diazirin-3-yl]-benzoic acid *N*-hydroxysuccinimide ester [TDBA-OSu] cross-linker. The Si−CH=CH−CH_3 surfaces thus offer a means of attaching a variety of chemical moieties to a silicon surface through a short linking group, enabling applications in molecular electronics, energy conversion, catalysis, and sensing.

1. Introduction

Densely packed organic layers bonded covalently to crystalline silicon (Si) surfaces without an interfacial silicon oxide (SiO_2) layer have received an increasing interest, mainly because of their variety of applications in micro- and nanoelectronics[1−8] as well as in (bio)chemical sensors.[9−16] Attachment of organic species on a Si substrate without intervening oxide could significantly reduce the density of trap states on Si surfaces.[17−19] Furthermore, it might potentially prevent diffusion of oxygen atoms into the monolayer/Si interface during either growth of insulating layer or postannealing process in the formation of high-dielectrics on Si.[20,21]

A variety of surface passivation methods have been investigated to preserve the nearly ideal electrical properties of the H-terminated Si(111) surfaces in ambient conditions.[22−24] The formation of Si−C bonds, however, has attracted a particular interest due to the kinetic inertness of these bonds as compared to Si−O or Si−H bonds. The Si−C bond is chemically more stable than Si−O bonds on oxidized Si surfaces and thus less susceptible to nucleophilic substitution reactions.[25] Si(111) surfaces have been functionalized by a variety of methods, including reaction with alkenes through a radical process catalyzed by a diacyl peroxide initiator,[26,27] use of UV[28−30] or

* To whom correspondence should be addressed. Phone: +972-4-8293087. Fax: +972-4-8295672.

(1) Barrelet, C. J.; Robinson, D. B.; Cheng, J.; Hunt, T. P.; Quate, C. F.; Chidsey, C. E. D. *Langmuir* **2001**, *17*, 3460–3465.
(2) Cheng, J.; Robinson, D. B.; Cicero, R. L.; Eberspacher, T.; Barrelet, C. J.; Chidsey, C. E. D. *J. Phys. Chem. B* **2001**, *105*, 10900–10904.
(3) Buriak, J. M. *Chem. Commun.* **1999**, 1051–1060.
(4) Wolkow, R. A. *Annu. Rev. Phys. Chem.* **1999**, *50*, 413–441.
(5) Cicero, R. L.; Linford, M. R.; Chidsey, C. E. D. *Langmuir* **2000**, *16*, 5688–5695.
(6) Terry, J.; Linford, M. R.; Wigren, C.; Cao, R. Y.; Pianetta, P.; Chidsey, C. E. D. *J. Appl. Phys.* **1999**, *85*, 213–221.
(7) Yamada, T.; Takano, N.; Yamada, K.; Yoshitomi, S.; Inoue, T.; Osaka, T. *J. Electroanal. Chem.* **2002**, *532*, 245–250.
(8) Yamada, T.; Inoue, T.; Yamada, K.; Takano, N.; Osaka, T.; Harada, H.; K. Nishiyama, K.; Taniguchi, I. *J. Am. Chem. Soc.* **2003**, *125*, 8039–8042.
(9) Yates, J. T., Jr. *Science* **1998**, *279*, 335–336.
(10) Wayner, D. D. M.; Wolkow, R. A. *J. Chem. Soc., Perkin Trans.* **2002**, *2*, 23–34.
(11) Buriak, J. M. *Chem. Rev.* **2002**, *102*, 1271–1308.
(12) Boukherroub, R.; Morin, S.; Wayner, D. D. M.; Bensebaa, F. G.; Sproule, I. J.; Baribeau, M.; Lockwood, D. J. *Chem. Mater.* **2001**, *13*, 2002–2011.
(13) Wojtyk, J. T. C.; Tomietto, M.; Boukherroub, R.; Wayner, D. D. M. *J. Am. Chem. Soc.* **2001**, *123*, 1535–1536.
(14) Bent, S. F. *J. Phys. Chem. B* **2002**, *106*, 2830–2842.
(15) Lasseter, T. L.; Clare, B. H.; Abbott, N. L.; Hamers, R. J. *J. Am. Chem. Soc.* **2004**, *126*, 10220–10221.
(16) Zhang, G.-J.; Chua, J. H.; Chee, R.-E.; Agarwal, A.; Wong, S. M.; Buddharaju, K. D.; Balasubramanian, N. *Biosens. Bioelectron* **2008**, *23*, 1701–1707.
(17) Webb, L. J.; Michalak, D. J.; Biteen, J. S.; Brunschwing, B. S.; Chan, A. S. Y.; Knapp, D. W.; Meyer, H. M.; Nemanick, E. J.; Traub, M. C.; Lewis, N. S. *J. Phys. Chem. B.* **2006**, *110*, 23450–23459.
(18) Buczkowski, A.; Radzimski, Z. J.; Rozgonyi, G. A.; Shimura, F. J. *Appl. Phys. Lett.* **1991**, *69*, 6495–6499.
(19) Liu, Y.-J.; Yu, H.-Z. *ChemPhysChem* **2002**, *3*, 799–802.
(20) Higashi, G. S.; Chabal, Y. J.; Trucks, G. W.; Raghavachari, K. *Appl. Phys. Lett.* **1990**, *56*, 656–658.
(21) Liu, Y.-J.; Yu, H.-Z. *J. Phys. Chem. B* **2003**, *107*, 7803–7811.
(22) Liu, Y.-J.; Yu, H.-Z. *ChemPhysChem* **2003**, *4*, 335–342.
(23) Chabal, Y.; Feldman, L. C. *Interface* **2005**, *14*, 31–40.
(24) Miramond, C.; Vuillaume, D. *J. Appl. Phys.* **2004**, *96*, 1529–1536.
(25) Faber, E. J.; de Smet, L. C. P. M.; Olthuis, W.; Zuilhof, H.; Sudhoelter, E. J. R.; Bergveld, P.; van den Berg, A. *ChemPhysChem* **2005**, *6*, 2153–2166.
(26) Linford, M. R.; Chidsey, C. E. D. *J. Am. Chem. Soc.* **1993**, *115*, 12631–12632.
(27) Linford, M. R.; Fenter, P.; Eisenberger, P. M.; Chidsey, C. E. D. *J. Am. Chem. Soc.* **1995**, *117*, 3145–3155.

10.1021/ja804674z CCC: $40.75

Nonequilibrium fluctuation-dissipation theorem of Brownian dynamics

L. Y. Chen[a)]
Department of Physics, University of Texas at San Antonio, San Antonio, Texas 78249, USA

(Received 21 August 2008; accepted 10 September 2008; published online 14 October 2008)

Studying the Brownian motion of a system driven by an external control from one macroscopic state to another macroscopic state, this paper presents the derivation of a nonlinear fluctuation-dissipation theorem (FDT). The new FDT relates the nonequilibrium work to the equilibrium free-energy difference in a very simple manner. It is valid wherever the Brownian dynamics is applicable. It recovers the well-known Crooks fluctuation theorem (CFT) within the quasiequilibrium regime where the dissipative work is nearly zero. It will also be shown that the CFT's fundamental assumption of microscopic reversibility is not obeyed in experiments such as mechanically unfolding biological molecules, in which the external driving forces depend on the system's coordinates. © *2008 American Institute of Physics.* [DOI: 10.1063/1.2992153]

The bridge from the nonequilibrium work to the equilibrium free-energy difference has been a subject of much interest in recent years. Such a bridge is necessary to relate the experimental data of forces and displacements to the intrinsic properties of the system in the unfolding studies of proteins and nucleic acids.[1] It also serves as an effective and efficient method in the computations of free energy.[2] In the current literature, Jarzynski equality[3] (JE) and the undergirding Crooks fluctuation theorem[4] (CFT) are taken as the bridge while questions have been raised[5–7] about their applicability and range of validity. The self-consistency check of the CFT has suggested[8] that the CFT and JE are valid only in the quasiequilibrium or linear response regime. In this paper, I will present the derivation of a new fluctuation-dissipation theorem (FDT) without invoking any assumption beyond the Brownian dynamics. I will also show that the assumption of microscopic reversibility, on which the CFT is based, is generally invalid outside the quasiequilibrium regime. This will establish that the CFT and JE are applicable only within the quasiequilibrium regime where the dissipative work is nearly zero. However, the new FDT is valid wherever the Brownian dynamics is applicable.

Let us start with the Langevin equation for the Brownian dynamics as follows:[9]

$$m_i\gamma\frac{dx_i}{dt}+\frac{\partial}{\partial x_i}V=F_i+\xi_i. \tag{1}$$

Here m_i and x_i are the atomic mass and coordinate of the ith degree of freedom, respectively. γ is the damping (frictional) constant. V is the potential energy of the system that is a function of all coordinates. ξ_i is the stochastic force acting on the ith degree of freedom. It is assumed to be Gaussian with the following characteristics:

$$\langle\xi_i(t)\rangle=0,\quad \langle\xi_i(t)\xi_j(t')\rangle=2m_i\gamma k_BT\delta_{ij}\delta(t-t'). \tag{2}$$

Here k_B is the Boltzmann constant. T is the absolute temperature. δ_{ij} is the Kronecker delta and $\delta(t-t')$ is the Dirac delta function. F_i is the external force component acting on the ith degree of freedom. The external force drives the system from state A at time $t=0$ to state B at time $t=\tau$. For example, in a mechanical unfolding experiment, the two terminus atoms are subject to the external forces that are functions of the atomic coordinates and time. In general, $F_i=F_i(x,t)$, where $x=\{x_i\}$ is the collection of the atomic coordinates.

Now, we divide the time interval $[0,\tau]$ into N equal slices of width $dt=\tau/N$. In this, we have $t_n=ndt$ with $n=0,1,\ldots,N$. For clarity, we omit the index for the degree of freedom and denote $x_n\triangleq x_i(t_n)$, $\partial V_n\triangleq\partial V(x(t_n))/\partial x_i$, and $F_n\triangleq F_i(x(t_n),t_n)$. Then the discrete form of the Langevin equation (1) is

$$m\gamma(x_{n+1}-x_n)+\partial V_n dt-F_n dt=\int_{t_n}^{t_{n+1}}dt'\,\xi(t'). \tag{3}$$

Noting the statistical characteristics of the stochastic term on the right hand side of Eq. (3), we have the transition probability between state x_n at time t_n and state x_{n+1} at time t_{n+1}, namely, the probability for the system to be in state x_{n+1} at time t_{n+1} given that it is in state x_n at time t_n as follows:

$$P(x_n,t_n|x_{n+1},t_{n+1})=\frac{1}{\Omega}\exp\left(-\frac{(m\gamma(x_{n+1}-x_n)+\partial V_n dt-F_n dt)^2}{4m\gamma k_BTdt}\right). \tag{4}$$

Here the normalization factor $\Omega=(2k_BTdt/m\gamma)^{1/2}$, which is independent of the system's coordinates. Note that the Ito scheme is adopted in this paper for the discrete form of the

a)Electronic mail: lychen@utsa.edu.

An efficient and exact stochastic simulation method to analyze rare events in biochemical systems

Hiroyuki Kuwahara[a] and Ivan Mura[b]
The Microsoft Research - University of Trento Centre for Computational and Systems Biology, Trento 38100, Italy

(Received 7 July 2008; accepted 28 August 2008; published online 22 October 2008)

In robust biological systems, wide deviations from highly controlled normal behavior may be rare, yet they may result in catastrophic complications. While *in silico* analysis has gained an appreciation as a tool to offer insights into system-level properties of biological systems, analysis of such rare events provides a particularly challenging computational problem. This paper proposes an efficient stochastic simulation method to analyze rare events in biochemical systems. Our new approach can substantially increase the frequency of the rare events of interest by appropriately manipulating the underlying probability measure of the system, allowing high-precision results to be obtained with substantially fewer simulation runs than the conventional direct Monte Carlo simulation. Here, we show the algorithm of our new approach, and we apply it to the analysis of rare deviant transitions of two systems, resulting in several orders of magnitude speedup in generating high-precision estimates compared with the conventional Monte Carlo simulation. © *2008 American Institute of Physics*. [DOI: 10.1063/1.2987701]

I. INTRODUCTION

While rare events are, by definition, ones that occur with extremely small probability, they can have significant influences and profound consequences in many systems.[1] This is particularly true in biochemical and physiological systems in that, while the occurrence of biochemical events that leads to some abnormal states may be rare, it can have devastating effects. For example, it has been shown that rare epigenetic modifications play crucial roles in the development of cancer cells by, among other things, inactivating tumor-suppressing genes.[2–5] The failed recognition of such dangerous cells by the immune system and the inability to induce apoptosis as a self-defense mechanism are another infrequent yet devastating event, potentially leading to growth and spread of tumors.[6] Thus, better understanding of the underlying biochemistry of such rare events is crucial, for example, to advancement of our knowledge on the development and physiology of diseases. Since computational methods come with virtually unlimited controllabilities and observabilities of biochemical systems, *in silico* analysis may provide a tool to shed some light on the mechanisms of physiologically relevant events that are rare yet catastrophic.

The most exact way to analyze a quantitative model of a biochemical system is *molecular dynamics*, where movements of every molecule are tracked.[7,8] The system state of molecular dynamics consists of the positions and the velocities of every molecule where the dynamics is described by capturing every movement and every collision of molecules. While this approach can describe the time evolution as well as the spatial distribution of each molecule, acquiring such detailed knowledge and performing such computationally expensive simulations may not be feasible. A more practical mathematical modeling formalism that can quantitatively capture rare dynamics based on deviant effects in biochemical systems is *stochastic chemical kinetics* (SCK).[9] SCK describes the time evolution of the molecular populations in a system through discrete and random reaction events by making the well-stirred (or spatial homogeneous) assumption. This assumption abstracts away the spatial property to greatly simplify the complexity of the system state description. While this simplification adds uncertainty in the dynamics of the system, SCK can correctly capture the temporal behavior of a well-stirred system in a probabilistic manner and the time evolution of the probability distribution of the system state is described by the *chemical master equation* (CME).[10,11] However, directly obtaining the solution of the CME of any realistic system, either analytically or numerically, is not feasible due to its intrinsic complexity. Thus, exact numerical realizations of a SCK model via the *stochastic simulation algorithm* (SSA) (Refs. 12 and 13) are often used to infer the temporal system behavior with a much smaller memory footprint.

Unfortunately, the computational requirements of the SSA can be substantial due to the fact that it requires a potentially large number of simulation runs in order to estimate the system behavior at a reasonable degree of statistical confidence. This problem becomes further pronounced in the analysis of rare events as it necessitates generation of a substantial number of sample trajectories. For example, the spontaneous, epigenetic switching rate from the lysogenic state to the lytic state in phage λ-infected *Escherichia coli*[14] is experimentally estimated to be in the order of 10^{-7} per cell per generation.[15] Thus, the SSA would expect to generate sample trajectories of this rare event only once every 10^7 runs, and it would require more than 10^{11} simulation runs to

[a]Electronic mail: kuwahara@cosbi.eu.
[b]Electronic mail: mura@cosbi.eu.

Lab on a Chip

RSC Publishing

Journals Lab on a Chip Advance Articles. DOI: 10.1039/b807682k

Lab Chip, 2009 | DOI: 10.1039/b807682k | Technical Note

Dynamic cell culture: a microfluidic function generator for live cell microscopy

Philip J. Lee *, Terry A. Gaige and Paul J. Hung

CellASIC Corporation, San Leandro, CA, USA. E-mail: pjlee@cellasic.com

Received 6th May 2008 , Accepted 18th August 2008

First published on the web 20th October 2008

We present a microfluidic system for time-lapsed, live cell microscopy with the ability to control solution exchange *via* a dynamic flow controller. The application specific microfluidic plates are designed to maintain adherent and non-adherent cell types for multiple days with continuous medium perfusion. Upstream channels with flow controlled *via* custom software allow the delivery of unique exposure profiles to the cultured cells, such as square waves, step functions, ramps, *etc.*

Introduction

The utilization of microfluidic devices for cell culture applications holds tremendous promise for the future of biology.[1] This approach enables the engineering of microenvironments at the cellular size scale[2] with miniaturization and automation of complex protocols.[3] In order to mimic the physiological environment of cells in tissues, a number of groups have successfully demonstrated the ability to create continuous flow arrays for *in vitro* microfluidic culture.[4–7] More recently, this capability was enhanced with systems capable of exposing cells to changing flow environments, enabling a type of "signal-response" experiment not previously possible.[8,9] Increased use of dynamic cell culture systems may provide novel insights into cellular processes that were not accessible with conventional static culture methods.

In this work, we describe the design and engineering of a robust microfluidic cell culture device with a straightforward interface for dynamic medium exposure. This concept is based on the use of disposable, application specific microfluidic plates and a universal flow control interface. The microfluidic plates house all sample solutions, media, and cells, and is formatted with a 96-well plate footprint, with 10 pipette accessible inlet/outlet well positions. Flows through the microfluidic device are actuated *via* precisely regulated pneumatic pressure routed to each of the 10 well positions.[9] The microfluidic cell culture chamber is based on previous work, with the key feature being a perfusion barrier to control nutrient transport and cell localization.[10] This design maintains the cultured cells in a specified imaging region with exposure to continuous perfusion of media solutions. A glass coverslide bottom and transparent optical path facilitate high magnification imaging on an inverted microscope.

Molecular Systems Biology 4; Article number 223; doi:10.1038/msb.2008.59
Citation: *Molecular Systems Biology* 4:223

www.molecularsystemsbiology.com

molecular systems biology

Transient transcriptional responses to stress are generated by opposing effects of mRNA production and degradation

Ophir Shalem[1,2], Orna Dahan[1], Michal Levo[1], Maria Rodriguez Martinez[1,3], Itay Furman[1], Eran Segal[2,*] and Yitzhak Pilpel[1,*]

[1] Department of Molecular Genetics, Weizmann Institute of Science, Rehovot, Israel, [2] Department of Applied Mathematics and Computer Science, Weizmann Institute of Science, Rehovot, Israel and [3] Department of Physics of Complex Systems, Weizmann Institute of Science, Rehovot, Israel
* Corresponding authors. Eran Segal, Department of Applied Mathematics and Computer Science, Weizmann Institute of Science, Herzel, Rehovot 76100, Israel Tel.: +972 8 934 4282; Fax: +972 8 934 4122; E-mail: Eran.Segal@weizmann.ac.il or Yitzhak Pilpe, Department of Molecular Genetics, Weizmann Institute of Science, Herzel, Rehovot 76100, Israel. Tel.: +972 8 934 6058; Fax: +972 8 934 4108; E-mail: pilpel@weizmann.ac.il

Received 14.5.08; accepted 14.9.08

The state of the transcriptome reflects a balance between mRNA production and degradation. Yet how these two regulatory arms interact in shaping the kinetics of the transcriptome in response to environmental changes is not known. We subjected yeast to two stresses, one that induces a fast and transient response, and another that triggers a slow enduring response. We then used microarrays following transcriptional arrest to measure genome-wide decay profiles under each condition. We found condition-specific changes in mRNA decay rates and coordination between mRNA production and degradation. In the transient response, most induced genes were surprisingly destabilized, whereas repressed genes were somewhat stabilized, exhibiting counteraction between production and degradation. This strategy can reconcile high steady-state level with short response time among induced genes. In contrast, the stress that induces the slow response displays the more expected behavior, whereby most induced genes are stabilized, and repressed genes are destabilized. Our results show genome-wide interplay between mRNA production and degradation, and that alternative modes of such interplay determine the kinetics of the transcriptome in response to stress.
Molecular Systems Biology 14 October 2008; doi:10.1038/msb.2008.59
Subject Categories: chromatin & transcription; RNA
Keywords: degradation; microarray; stress; transcription; yeast

Introduction

In response to environmental stimuli, the mRNA abundance of a large fraction of the genome changes either by increasing or decreasing its levels (Gasch *et al*, 2000, 2001; Jelinsky *et al*, 2000; Gasch and Werner-Washburne, 2002). Clearly, to understand the state of the transcriptome under varying conditions, the role of both mRNA production and degradation must be examined. An increase in mRNA abundance in response to a stimulus may be achieved either by increasing the rate of transcription or by decreasing the rate of degradation. Likewise, a decrease in the transcript level can be achieved either by an increase in the rate of degradation or a decrease in the rate of production. More complex interplays between production and degradation are also possible. For instance, an increase in mRNA production rate might be accompanied by a decrease in degradation rate, leading to mRNA accumulation. Perhaps less intuitive is the possibility that an increase in transcript levels would be obtained by increasing both production and degradation rates, provided that the extent of production increase exceeds the elevation in the degradation rate (Box 1A). Whereas steady-state levels are simply determined by the ratio of production and degradation rates, the kinetic behavior is expected to be more complex, which is dependent on the actual rates, and hence different under the above regimens (Box 1B).

As a result, one may expect complex regimens of interplay between transcription induction and repression, and stabilization versus destabilization of mRNAs that will result in various effects on response kinetics (Perez-Ortin *et al*, 2007). Yet customary transcript abundance measurements, e.g. with microarrays, provide only the net values and do not provide information regarding the relative contribution of mRNA production and degradation.

Although still scarce when compared to transcription, the attention directed toward the control of mRNA degradation has

Molecular Systems Biology 4; Article number 221; doi:10.1038/msb.2008.58
Citation: *Molecular Systems Biology* 4:221

www.molecularsystemsbiology.com

molecular systems biology

A quantitative comparison of sRNA-based and protein-based gene regulation

Pankaj Mehta[1,3,*], Sidhartha Goyal[2,3,*] and Ned S Wingreen[1]

[1] Department of Molecular Biology, Princeton University, Princeton, NJ, USA and [2] Department of Physics, Princeton University, Princeton, NJ, USA
[3] These authors contributed equally to this work
* Corresponding authors. P Mehta, Department of Molecular Biology, Princeton University, Princeton, NJ 08544, USA. Tel.: +1 609 258 8696; Fax: +1 609 258 8616; E-mail: pmehta@princeton.edu or S Goyal, Department of Physics, Princeton University, Jadwin Hall, Washington Road, Princeton, NJ 08544, USA. Tel.: +1 609 240 9316; Fax: +1 609 258 8616; E-mail: goyal@princeton.edu

Received 12.3.08; accepted 5.9.08

Small non-coding RNAs (sRNAs) have important functions as genetic regulators in prokaryotes. sRNAs act post-transcriptionally through complementary pairing with target mRNAs to regulate protein expression. We use a quantitative approach to compare and contrast sRNAs with conventional transcription factors (TFs) to better understand the advantages of each form of regulation. In particular, we calculate the steady-state behavior, noise properties, frequency-dependent gain (amplification), and dynamical response to large input signals of both forms of regulation. Although the mean steady-state behavior of sRNA-regulated proteins exhibits a distinctive tunable threshold linear behavior, our analysis shows that transcriptional bursting leads to significantly higher intrinsic noise in sRNA-based regulation than in TF-based regulation in a large range of expression levels and limits the ability of sRNAs to perform quantitative signaling. Nonetheless, we find that sRNAs are better than TFs at filtering noise in input signals. Additionally, we find that sRNAs allow cells to respond rapidly to large changes in input signals. These features suggest a 'niche' for sRNAs in allowing cells to transition quickly yet reliably between distinct states. This functional niche is consistent with the widespread appearance of sRNAs in stress response and quasi-developmental networks in prokaryotes.
Molecular Systems Biology 14 October 2008; doi:10.1038/msb.2008.58
Subject Categories: RNA; metabolic and regulatory networks; signal transduction
Keywords: biophysics; genetic networks; signal processing; small RNA

Introduction

It is now clear that small non-coding RNAs (sRNAs) have a crucial function in prokaryotic gene regulation as both positive and negative regulators. sRNAs are involved in many biological functions, including quorum sensing (Fuqua *et al*, 2001; Lenz *et al*, 2004), stress response and virulence factor regulation (Gottesman, 2004; Storz *et al*, 2004, 2005; Majdalani *et al*, 2005; Gottesman *et al*, 2006), and the regulation of outer membrane proteins (Guillier *et al*, 2006; Vogel and Papenfort, 2006). One major class of prokaryotic sRNAs (antisense sRNAs) negatively regulates proteins by destabilizing the target protein's mRNA (Figure 1). These ~100 bp antisense sRNAs prevent translation by binding to the target mRNAs in a process mediated by the RNA chaperone Hfq (Gottesman, 2004; Lenz *et al*, 2004). On binding, both the mRNAs and sRNAs are degraded (Gottesman, 2004), suggesting that prokaryotic sRNAs—unlike their eukaryotic counterparts—act stoichiometrically on their targets. Other antisense sRNAs positively regulate protein expression by promoting ribosome binding to target mRNAs, also in a stoichiometric manner (Gottesman, 2004).

Although transcription factor (TF)-based regulation is ubiquitous in prokaryotic gene circuits (Ptashne and Gann, 2001), thus far sRNAs have largely been found in circuits responding to strong environmental cues (e.g. extreme nutrient limitation). This leads to a natural question: are transcriptional regulation by TFs and post-transcriptional regulation by sRNAs distinctly well suited for different biological tasks?

To address this question, we report a quantitative comparison of the signaling properties of TF- and sRNA-based gene regulation. In general, a signaling system can be characterized by how it processes different types of inputs. We therefore treat TF- and sRNA-based regulation as signal processing systems with an input signal—the average concentration of the TFs

Molecular Systems Biology 4; Article number 220; doi:10.1038/msb.2008.57
Citation: *Molecular Systems Biology* 4:220

www.molecularsystemsbiology.com

molecular systems biology

An integrated cell-free metabolic platform for protein production and synthetic biology

Michael C Jewett[1,3], Kara A Calhoun[1], Alexei Voloshin[1], Jessica J Wuu[1] and James R Swartz[1,2,*]

[1] Department of Chemical Engineering, Stanford University, Stanford, CA 94305-5025, USA and [2] Department of Bioengineering, Stanford University, Stanford, CA 94305-5444, USA
[3] Present address: Department of Genetics, Harvard Medical School, Boston, MA 02115, USA
* Corresponding author. Department of Chemical Engineering, Stanford University, Stauffer III, Rm 113, Stanford, CA 94305-5025, USA. Tel.: +1 650 723 5398; Fax: +1 650 725 0555; E-mail: jswartz@stanford.edu

Received 23.5.08; accepted 20.8.08

Cell-free systems offer a unique platform for expanding the capabilities of natural biological systems for useful purposes, i.e. synthetic biology. They reduce complexity, remove structural barriers, and do not require the maintenance of cell viability. Cell-free systems, however, have been limited by their inability to co-activate multiple biochemical networks in a single integrated platform. Here, we report the assessment of biochemical reactions in an *Escherichia coli* cell-free platform designed to activate natural metabolism, the Cytomim system. We reveal that central catabolism, oxidative phosphorylation, and protein synthesis can be co-activated in a single reaction system. Never before have these complex systems been shown to be simultaneously activated without living cells. The Cytomim system therefore promises to provide the metabolic foundation for diverse *ab initio* cell-free synthetic biology projects. In addition, we describe an improved Cytomim system with enhanced protein synthesis yields (up to 1200 mg/l in 2 h) and lower costs to facilitate production of protein therapeutics and biochemicals that are difficult to make *in vivo* because of their toxicity, complexity, or unusual cofactor requirements.

Molecular Systems Biology 14 October 2008; doi:10.1038/msb.2008.57
Subject Categories: synthetic biology; cellular metabolism
Keywords: cell-free biology; *in vitro* translation; oxidative phosphorylation; protein synthesis; synthetic biology

Introduction

Cell-free systems provide a valuable platform for understanding, using, and expanding the capabilities of natural systems (Forster and Church, 2006, 2007; Swartz, 2006; Doktycz and Simpson, 2007; Meyer *et al*, 2007). As a complement to *in vivo*-based approaches, cell-free systems have the advantage of offering direct access to complex biological processes. New components (natural and non-natural) can be added or synthesized and can be maintained at precise ratios. The chemical environment can be controlled, actively monitored, and rapidly sampled. Moreover, systemic responses to environmental stimuli are minimized and high efficiency is afforded by directing resources toward exclusive user-defined objectives.

Cell-free protein synthesis (CFPS) systems, based on crude extracts, are one of the most prominent examples of cell-free biology. They were used in the pioneering studies of Nirenberg and Matthaei (1961) and played an essential role in deciphering the genetic code (Nirenberg, 2004). More recently, CFPS has shown remarkable utility as a protein synthesis technology (Katzen *et al*, 2005; Swartz, 2006), including the production of patient-specific vaccine candidates (Yang *et al*, 2005; Kanter *et al*, 2007) and pharmaceutical proteins (Yang *et al*, 2005; Goerke and Swartz, 2008). To test and model our understanding of how biology works, constructive cell-free approaches have also been reported. Shimizu *et al* (2001) reconstituted all of the factors necessary for protein synthesis from purified components. Additionally, genetic circuits have been built in crude extracts (Noireaux *et al*, 2003) and also from individual macromolecules (Kim *et al*, 2006).

Despite being used for decades as a tool in fundamental and applied research, one major disadvantage of most cell-free systems is their inability to co-activate multiple complex biochemical networks in a single integrated platform. To address this challenge, we sought to create a useful and cost-effective cell-free system that co-activates central metabolism, oxidative phosphorylation, transcription, translation, and

Molecular Microbiology (2008) 70(2), 369–378 ■

doi:10.1111/j.1365-2958.2008.06412.x
First published online 29 August 2008

General stress response signalling: unwrapping transcription complexes by DNA relaxation via the sigma38 C-terminal domain

Yi-Xin Huo, Adam Z. Rosenthal and Jay D. Gralla*
Department of Chemistry and Biochemistry and the Molecular Biology Institute, University of California, PO Box 951569, Los Angeles, CA 90095, USA.

Summary

***Escherichia coli* responds to stress by a combination of specific and general transcription signalling pathways. The general pathways typically require the master stress regulator sigma38 (rpoS). Here we show that the signalling from multiple stresses that relax DNA is processed by a non-conserved eight-amino-acid tail of the sigma 38 C-terminal domain. By contrast, responses to two stresses that accumulate potassium glutamate do not rely on this short tail, but still require the overall C-terminal domain. *In vitro* transcription and footprinting studies suggest that multiple stresses can target a poised RNA polymerase and activate it by unwrapping DNA from a nucleosome-like state, allowing the RNA polymerase to escape into productive mode. This transition can be accomplished by either the DNA relaxation or potassium glutamate accumulation that characterizes many stresses.**

Introduction

In its natural environments *Escherichia coli* must deal with many stresses, often simultaneously. These include the gastric stomach of certain hosts, the high osmotic pressure of the lower gastrointestinal tract and other saline environments, extreme heat and cold, radiation challenges and frequent nutritional limitation (Hengge-Aronis, 2002). The bacterium has evolved specific pathways that produce defined sets of protective proteins tailored for each challenge. These pathways are mostly mediated by transcription factors (Giuliodori *et al.*, 2007). Such factors include macromolecules such as activators, repressors and sigma factors, the latter for example for heat shock (Yura *et al.*, 2007). The cell also uses small molecules to directly influence RNA polymerase in response to certain stresses. These include ppGpp for general nutritional stress (Gralla, 2005), glutamate for osmotic stress (Lee and Gralla, 2004) and acetate for volatile fatty acid stress (Rosenthal *et al.*, 2006; 2008a). The protective proteins produced by these various pathways include both unique and overlapping species (Weber *et al.*, 2005).

In addition, *E. coli* and related bacteria have a general stress response. This is mediated by the general stress regulator sigma38 (rpoS, sigmaS) (Hengge-Aronis, 2002). Sigma38 levels are low in the rare stress-free environment and become higher in response to most stresses (Hengge-Aronis, 1996). After it accumulates sigma38 binds a fraction of the common core RNA polymerase and transcribes two sets of protective genes, those specific for the inducing stress and also for general stress-adaptive proteins (Weber *et al.*, 2005). The promoters for all of these protective genes include DNA elements that favour transcription by the sigma38 holoenzyme (Lee and Gralla, 2001; Typas *et al.*, 2007). A number of these genes rely on promoter-specific DNA binding regulators, which typically associate with upstream elements to assist in transcription in response to specific stresses (Sayed *et al.*, 2007). However, no individual DNA binding regulator is responsible for the general stress response.

A well-studied general stress factor is the periplasmic protein *osmY* (Yim *et al.*, 1994). Although originally studied in the context of osmotic stress (Ding *et al.*, 1995), *osmY* is generally stress-induced, for example by heat (Muffler *et al.*, 1997), cold (Jones *et al.*, 2006), acetate (Arnold *et al.*, 2001) and acid stresses as well as during entry into stationary phase (Weber *et al.*, 2005). In the absence of stress the *osmY* gene is silent, even when sigma38 is present. Under such conditions the *osmY* promoter can be occupied by sigma38 RNA polymerase, but the transcription complex is not active (Rosenthal *et al.*, 2008b). In the case of osmotic stress the activating event is believed to be the accumulation of potassium glutamate. This has been reproduced *in vitro* on supercoiled DNA; the transcription complex is maintained in an apparently wrapped inactive state and then potassium glutamate unwraps the sigma38 RNA polymerase as

Accepted 10 August, 2008. *For correspondence. E-mail gralla@chem.ucla.edu; Tel. (+1) 310 825 1620; Fax (+1) 310 206 4038.

Molecular Microbiology (2008) 70(3), 682–694

doi:10.1111/j.1365-2958.2008.06438.x
First published online 29 September 2008

Localization of general and regulatory proteolysis in *Bacillus subtilis* cells

Janine Kirstein,[1†] Henrik Strahl,[2] Noël Molière,[1] Leendert W. Hamoen[2*] and Kürşad Turgay[1]**

[1]*Institut für Biologie – Mikrobiologie, FU Berlin, Königin-Luise-Str. 12-16, 14195 Berlin, Germany.*

[2]*Institute for Cell and Molecular Biosciences, Newcastle University, Framlington Place, Newcastle NE2 4HH, UK.*

Summary

Protein degradation mediated by ATP-dependent proteases, such as Hsp100/Clp and related AAA+ proteins, plays an important role in cellular protein homeostasis, protein quality control and the regulation of, e.g. heat shock adaptation and other cellular differentiation processes. ClpCP with its adaptor proteins and other related proteases, such as ClpXP or ClpEP of *Bacillus subtilis*, are involved in general and regulatory proteolysis. To determine if proteolysis occurs at specific locations in *B. subtilis* cells, we analysed the subcellular distribution of the Clp system together with adaptor and general and regulatory substrate proteins, under different environmental conditions. We can demonstrate that the ATPase and the proteolytic subunit of the Clp proteases, as well as the adaptor or substrate proteins, form visible foci, representing active protease clusters localized to the polar and to the mid-cell region. These clusters could represent a compartmentalized place for protein degradation positioned at the pole close to where most of the cellular protein biosynthesis and also protein quality control are taking place, thereby spatially separating protein synthesis and degradation.

Introduction

Protein degradation plays an important role in protein homeostasis and in protein quality control. Together with molecular chaperone systems, proteases ensure the proper function of proteins in their cellular environment (Hartl and Hayer-Hartl, 2002; Bukau *et al.*, 2006). Proteolysis is also used for regulatory purposes, such as the regulated degradation of key transcription factors that control cell cycle, developmental or adaptation processes (Ciechanover, 1998; Gottesman, 2003; Jenal and Hengge-Aronis, 2003; Pickart and Cohen, 2004).

Both general and regulatory proteolysis are mediated by dedicated molecular machines, which are ATP-dependent proteases consisting of ring-forming hexameric Hsp100/Clp proteins of the AAA+ family, associated on both sides of the barrel-forming peptidases complex. The AAA+ proteins of the protease can recognize, unfold and translocate proteins into the proteolytic chamber of the interacting peptidase compartment (Lupas *et al.*, 1997; Wickner *et al.*, 1999; Pickart and Cohen, 2004; Sauer *et al.*, 2004). An example of such proteases in eukaryotes is the proteasome (Ciechanover, 1998; Pickart and Cohen, 2004). In prokaryotic cells, homologous protease complexes are formed by the AAA+ proteins ClpA, ClpX or ClpC, which assemble with the peptidase ClpP (Wickner *et al.*, 1999; Sauer *et al.*, 2004). Relatively little is known concerning the subcellular localization of these protease systems, their substrates and other components of the protein quality control system (Wojcik and DeMartino, 2003; Lindner *et al.*, 2008), even though this information is important for a full comprehension of the diverse and important intracellular processes involving proteolysis and protein quality control (Balch *et al.*, 2008).

We use the model organism *Bacillus subtilis* to investigate the dynamic subcellular localization of the Hsp100/Clp protease systems. Cells of a *B. subtilis* population can adapt and react to a wide array of environmental changes by, e.g. heat shock and general stress adaptation (Hecker *et al.*, 2007), and developmental processes, such as sporulation (Rudner and Losick, 2001) or competence development (Chen *et al.*, 2005).

The *B. subtilis* Hsp100/Clp proteins ClpC, ClpE and ClpX associate with ClpP to form protease complexes. Of these three Hsp100/Clp proteins, ClpX is the most abundant Clp ATPase under normal growth conditions (Gerth *et al.*, 2004). ClpC and ClpX are intricately involved in both general protein quality control (Krüger *et al.*, 1994; 2000; Wiegert and Schumann, 2001; Schlothauer *et al.*,

Accepted 29 August, 2008. For correspondence. *E-mail l.hamoen@ncl.ac.uk; Tel. (+44) 191 2228983; Fax (+44) 191 2227424; **E-mail kturgay@zedat.fu-berlin.de; Tel. (+49) 30 83853111; Fax (+49) 30 83853118. †Present address: Department of Biochemistry, Molecular Biology and Cell Biology, Northwestern University, 205 Tech Drive, Hogan 2-100, Evanston, IL 60208, USA.

Molecular Microbiology (2008) 70(4), 1012–1025 ■

doi:10.1111/j.1365-2958.2008.06467.x
First published online 8 October 2008

Inducible protein degradation in *Bacillus subtilis* using heterologous peptide tags and adaptor proteins to target substrates to the protease ClpXP

Kevin L. Griffith and Alan D. Grossman*
Department of Biology, Massachusetts Institute of Technology, Cambridge, MA 02139, USA.

Summary

The ability to manipulate protein levels is useful for dissecting regulatory pathways, elucidating gene function and constructing synthetic biological circuits. We engineered an inducible protein degradation system for use in *Bacillus subtilis* based on *Escherichia coli* and *Caulobacter crescentus* ssrA tags and SspB adaptors that deliver proteins to ClpXP for proteolysis. In this system, modified *ssrA* degradation tags are fused onto the 3′ end of the genes of interest. Unlike wild-type ssrA, these modified tags require the adaptor protein SspB to target tagged proteins for proteolysis. In the absence of SspB, the tagged proteins accumulate to near physiological levels. By inducing SspB expression from a regulated promoter, the tagged substrates are rapidly delivered to the *B. subtilis* ClpXP protease for degradation. We used this system to degrade the reporter GFP and several native *B. subtilis* proteins, including, the transcription factor ComA, two sporulation kinases (KinA, KinB) and the sporulation and chromosome partitioning protein Spo0J. We also used modified *E. coli* and *C. crescentus* ssrA tags to independently control the degradation of two different proteins in the same cell. These tools will be useful for studying biological processes in *B. subtilis* and can potentially be modified for use in other bacteria.

Introduction

The ability to experimentally manipulate protein levels within the cell is useful for studying biological processes. Protein levels are typically manipulated by overexpressing or deleting the gene encoding the protein of interest. In the case of essential genes, conditional alleles, including those that regulate transcription of the gene of interest thereby allowing expression to be turned off or down, and temperature sensitive (ts) mutations, are used to reduce or eliminate function. Transcriptional depletion studies can be problematic due to the time required to sufficiently reduce pre-existing protein levels, and isolating ts alleles is often laborious and involves extensive characterization of isolated mutants. In eukaryotes, an N-terminal tag that confers temperature induced degradation has been used widely to selectively inactivate proteins of interest (Dohmen *et al.*, 1994; Dohmen and Varshavsky, 2005; Dohmen, 2006).

We constructed an inducible degradation system in *Bacillus subtilis* by modifying the *Escherichia coli* and *Caulobacter crescentus* ssrA degradation signals. Many bacteria (Gueneau de Novoa and Williams, 2004) use the ssrA or tmRNA (combined transfer and messenger RNA) tagging system for rescuing stalled ribosomes and targeting polypeptides for degradation. When a ribosome stalls on an mRNA, tmRNA can enter the ribosome leading to the addition of amino acids, the ssrA tag, onto the C-terminus of the nascent polypeptide. The ssrA tag enables the ribosome to terminate translation and disengage the polypeptide, while simultaneously providing a mechanism for clearing truncated polypeptides from the cell by targeting them for degradation by the highly conserved protease ClpXP (Tu *et al.*, 1995; Keiler *et al.*, 1996; Gottesman *et al.*, 1998; Moore and Sauer, 2007). The last three amino acids of the ssrA tag (LAA) are highly conserved and comprise the ClpX-recognition sequence (Flynn *et al.*, 2001; Wiegert and Schumann, 2001; Gueneau de Novoa and Williams, 2004; Chien *et al.*, 2007a; Lessner *et al.*, 2007; Fig. 1A).

In some cases, an adaptor protein, e.g. SspB in *E. coli* and *C. cresentus*, interacts with sequences in the ssrA tag upstream of the ClpX-recognition element (Fig. 1A) and tethers tagged substrates to ClpX to aid in degradation (Chien *et al.*, 2007a; Lessner *et al.*, 2007; Levchenko *et al.*, 2000). The SspB-recognition sequence in ssrA is less conserved than the ClpX-recognition sequence, allowing for specific interactions between ssrA and its cognate SspB adaptor (Flynn *et al.*, 2001; Gueneau de Novoa and Williams, 2004; Chien *et al.*, 2007b; Fig. 1A).

Accepted 17 September, 2008. *For correspondence. E-mail adg@mit.edu; Tel. (+1) 617 253 1515; Fax (+1) 617 253 2643.

Interconvertible Lac Repressor–DNA Loops Revealed by Single-Molecule Experiments

Oi Kwan Wong[1], Martin Guthold[2], Dorothy A. Erie[3], Jeff Gelles[1*]

1 Department of Biochemistry, Brandeis University, Waltham, Massachusetts, United States of America, 2 Department of Physics, Wake Forest University, Winston-Salem, North Carolina, United States of America, 3 Department of Chemistry and Curriculum Applied and Materials Sciences, University of North Carolina at Chapel Hill, Chapel Hill, North Carolina, United States of America

At many promoters, transcription is regulated by simultaneous binding of a protein to multiple sites on DNA, but the structures and dynamics of such transcription factor-mediated DNA loops are poorly understood. We directly examined in vitro loop formation mediated by *Escherichia coli* lactose repressor using single-molecule structural and kinetics methods. Small (~150 bp) loops form quickly and stably, even with out-of-phase operator spacings. Unexpectedly, repeated spontaneous transitions between two distinct loop structures were observed in individual protein–DNA complexes. The results imply a dynamic equilibrium between a novel loop structure with the repressor in its crystallographic "V" conformation and a second structure with a more extended linear repressor conformation that substantially lessens the DNA bending strain. The ability to switch between different loop structures may help to explain how robust transcription regulation is maintained even though the mechanical work required to form a loop may change substantially with metabolic conditions.

Citation: Wong OK, Guthold M, Erie DA, Gelles J (2008) Interconvertible Lac repressor–DNA loops revealed by single-molecule experiments. PLoS Biol 6(9): e232. doi:10.1371/journal.pbio.0060232

Introduction

DNA looping, in which a protein or protein complex interacts simultaneously with two separated sites on a DNA molecule, is a recurring theme in transcription regulation [1]. A prototypical example is transcription initiation at the *E. coli lacZYA* promoter, which is modulated through DNA looping by the lactose repressor. The promoter vicinity includes three operator sites: a primary operator (O_1) located 11 bp downstream from the *lacZ* transcription start site, and two auxiliary operators (O_2 and O_3) with lower affinities for the repressor located 401 bp downstream and 92 bp upstream of O_1, respectively (see review [2]). Repressor binding to O_1 blocks transcription from the *lacZYA* promoter. Nevertheless, the presence of O_2 and O_3 is indispensable for complete transcriptional repression in wild-type bacterial strains because the repressor loops DNA by binding simultaneously to O_1 and O_2 or O_3 [3–6], and such looping enhances repression by increasing the occupancy of O_1 by repressor [5,7].

In many transcription factors that function at least in part by DNA looping (for example, the lambda, ara, and gal repressors [8–10]), the protein complex interacts with two binding sites displayed on the same face of the double helix. Both in vitro and in vivo, these systems display a characteristic dependence of repression on interoperator spacing, with strong repression when operators are separated by an integer number of helical repeats ("in phase"), and repression weak or absent when an additional half turn of the helix is added ("out of phase") [9,11–14]. The reduced repression with out-of-phase operators is consistent with simple models of DNA elasticity, which predict a substantial energy cost to twist a short interoperator DNA segment by a half turn. In contrast, the effects of operator phasing on DNA looping by Lac repressor are in general weaker than those seen with other well-characterized bacterial repressors. Also, there is strong evidence from studies in vitro ([15,16] and references therein) and in vivo [17] that stable looped repressor–DNA complexes can form with operator spacings as small as or smaller than the 92-bp O_1–O_3 spacing. Even spacing the operators so that they are positioned on opposite sides of the double helix only 14.5 and 15.5 turns apart, so that substantial DNA twisting and bending may be required to close the loop, allows formation of putatively looped species, apparently with only a modest reduction in stability relative to similarly sized in-phase loops [15]. Out-of-phase operator spacings of similar size also give levels of repression in vivo consistent with looping [18].

No direct determinations of the structures of small Lac repressor–DNA looped complexes are available. The availability of crystallographic structures for the repressor alone and in complex with two DNA oligonucleotides [19,20], together with studies of the thermodynamic and kinetic stabilities of Lac repressor–DNA looped complexes in vitro [7,21–25], have led to the proposal of a variety of different structural models for looped protein–DNA complexes [1,19,20,24,26–28]. Most of these models are based on the crystallographic repressor–oligonucleotide model and a smoothly bent interoperator DNA segment. However, the tightly bent or strongly twisted interoperator DNA in these models is predicted to be highly energetically unfavorable

Academic Editor: Daniel Herschlag, Stanford University, United States of America

Received May 3, 2008; **Accepted** August 13, 2008; **Published** September 30, 2008

Abbreviations: AFM, atomic force microscopy; TPM, tethered particle motion; WLC, worm-like chain

* To whom correspondence should be addressed. E-mail: gelles@brandeis.edu

The NDR/LATS Family Kinase Cbk1 Directly Controls Transcriptional Asymmetry

Emily Mazanka[1], Jess Alexander[2], Brian J. Yeh[1], Patrick Charoenpong[1], Drew M. Lowery[2], Michael Yaffe[2], Eric L. Weiss[1*]

1 Department of Biochemistry, Molecular Biology, and Cell Biology, Northwestern University, Evanston, Illinois, United States of America, 2 Department of Biology and Biological Engineering, Massachusetts Institute of Technology, Cambridge, Massachusetts, United States of America.

Cell fate can be determined by asymmetric segregation of gene expression regulators. In the budding yeast *Saccharomyces cerevisiae*, the transcription factor Ace2 accumulates specifically in the daughter cell nucleus, where it drives transcription of genes that are not expressed in the mother cell. The NDR/LATS family protein kinase Cbk1 is required for Ace2 segregation and function. Using peptide scanning arrays, we determined Cbk1's phosphorylation consensus motif, the first such unbiased approach for an enzyme of this family, showing that it is a basophilic kinase with an unusual preference for histidine −5 to the phosphorylation site. We found that Cbk1 phosphorylates such sites in Ace2, and that these modifications are critical for Ace2's partitioning and function. Using proteins marked with GFP variants, we found that Ace2 moves from isotropic distribution to the daughter cell nuclear localization, well before cytokinesis, and that the nucleus must enter the daughter cell for Ace2 accumulation to occur. We found that Cbk1, unlike Ace2, is restricted to the daughter cell. Using both in vivo and in vitro assays, we found that two critical Cbk1 phosphorylations block Ace2's interaction with nuclear export machinery, while a third distal modification most likely acts to increase the transcription factor's activity. Our findings show that Cbk1 directly controls Ace2, regulating the transcription factor's activity and interaction with nuclear export machinery through three phosphorylation sites. Furthermore, Cbk1 exhibits a novel specificity that is likely conserved among related kinases from yeast to metazoans. Cbk1 is functionally restricted to the daughter cell, and cannot diffuse from the daughter to the mother. In addition to providing a mechanism for Ace2 segregation, these findings show that an isotropically distributed cell fate determinant can be asymmetrically partitioned in cytoplasmically contiguous cells through spatial segregation of a regulating protein kinase.

Citation: Mazanka E, Alexander J, Yeh BJ, Charoenpong P, Lowery DM, et al. (2008) The NDR/LATS family kinase Cbk1 directly controls transcriptional asymmetry. PLoS Biol 6(8): e203. doi:10.1371/journal.pbio.0060203

Introduction

Cells can adopt divergent fates upon division by unequally distributing molecules or structures that direct distinct gene expression programs. The genesis of this asymmetry rests on the cell's underlying architecture, and can involve segregation of mRNAs, transcription factors, and cell surface receptors [1,2]. Unquestionably critical for metazoan development, asymmetric gene expression is also important in unicellular eukaryotes. In the budding yeast *Saccharomyces cerevisiae*, for example, unequal partitioning of specific transcription factors causes mother and daughter cells to express different genes late in division [3–7].

Asymmetry of intracellular cell fate determinants requires their physical segregation as well as a mechanism to ensure that they do not act before the differentiating cells are functionally separated. In a number of well-characterized cases, transcriptional regulators are directly partitioned by cytoskeleton-associated machinery.

In *Drosophila melanogaster*, differentiation of neuroblasts and ganglion mother cells (GMCs) is achieved through asymmetric segregation of the transcription factor Prospero's protein and mRNA, in association with the adaptor proteins Miranda and Staufen [8–10]. Miranda's segregation to the cortex of the presumptive GMC involves the actin cytoskeleton and the opposing activities of myosin VI and myosin II; this is mitotically regulated by the anaphase-promoting complex/cyclosome [11]. In the next cell cycle, Prospero translocates to the GMC nucleus, where it regulates transcription of GMC-specific genes. In budding yeast, daughter cells are prevented from switching mating types by the asymmetrically segregated transcriptional repressor Ash1. This partitioning also depends on the actin cytoskeleton: *ASH1* mRNA is transported by a class V myosin to the bud tip during mitosis and tethered to the daughter cell cortex. It remains there until the beginning of the next cell cycle, whereupon it is translated to produce the Ash1 repressor protein [4–6].

Asymmetric gene expression is also important in the last step of budding yeast cell division, but is generated by a different mechanism. Final separation of mother and daughter yeast cells requires removal of a chitin-rich septum constructed between the cells during cytokinesis [12]. Destruction of this septum occurs from the daughter side. This asymmetry is due to a daughter-specific transcriptional program driven by the transcriptional activator Ace2, which

Academic Editor: David Pellman, Dana-Farber Cancer Institute, United States of America

Received April 22, 2008; **Accepted** July 14, 2008; **Published** August 19, 2008

Abbreviations: CDK, cyclin-dependent kinase; ChIP, chromatin immunoprecipitation; GMC, ganglion mother cells; LMB, leptomycin B; NES, nuclear export sequence; RAM, Regulation of Ace2 and Morphogenesis; RT-PCR, real-time polymerase chain reaction

* To whom correspondence should be addressed. E-mail: elweiss@northwestern.edu

A genetic timer through noise-induced stabilization of an unstable state

Marc Turcotte*, Jordi Garcia-Ojalvo†, and Gürol M. Süel*‡§

*Department of Pharmacology, University of Texas Southwestern Medical Center, Dallas, TX 753903; †Departament de Física i Enginyeria Nuclear, Universitat Politècnica de Catalunya, Colom 11, E-08222 Terrassa, Spain; and ‡Green Center for Systems Biology, University of Texas Southwestern Medical Center, Dallas, TX 75390

Edited by José N. Onuchic, University of California at San Diego, La Jolla, CA, and approved August 27, 2008 (received for review July 1, 2008)

Stochastic fluctuations affect the dynamics of biological systems. Typically, such noise causes perturbations that can permit genetic circuits to escape stable states, triggering, for example, phenotypic switching. In contrast, studies have shown that noise can surprisingly also generate new states, which exist solely in the presence of fluctuations. In those instances noise is supplied externally to the dynamical system. Here, we present a mechanism in which noise intrinsic to a simple genetic circuit effectively stabilizes a deterministically unstable state. Furthermore, this noise-induced stabilization represents a unique mechanism for a genetic timer. Specifically, we analyzed the effect of noise intrinsic to a prototypical two-component gene-circuit architecture composed of interacting positive and negative feedback loops. Genetic circuits with this topology are common in biology and typically regulate cell cycles and circadian clocks. These systems can undergo a variety of bifurcations in response to parameter changes. Simulations show that near one such bifurcation, noise induces oscillations around an unstable spiral point and thus effectively stabilizes this unstable fixed point. Because of the periodicity of these oscillations, the lifetime of the noise-dependent stabilization exhibits a polymodal distribution with multiple, well defined, and regularly spaced peaks. Therefore, the noise-induced stabilization presented here constitutes a minimal mechanism for a genetic circuit to function as a timer that could be used in the engineering of synthetic circuits.

bifurcation | dynamics | circuit | stochastic | quantized cycle

Stochastic fluctuations in gene expression and protein concentrations are a natural by-product of biochemical reactions in cells. Properties of this biochemical noise within genetic circuits, such as their amplitude, distribution, and propagation, have been extensively characterized (1–9). Additionally, theoretical and experimental studies have established that such noise can induce stochastic switching between distinct and stable phenotypic states (5, 10–23). Noise within genetic circuits is therefore thought to contribute to phenotypic heterogeneity in genetically identical cellular populations. It has also recently been shown experimentally that noise can trigger cellular differentiation in fruit flies and bacteria (14, 17, 18, 24). Together, these studies establish that noise can play an active functional role in cellular processes by effectively destabilizing and thus inducing escape from stable phenotypic states.

Besides its common role in destabilizing stable states, noise can also have the more counterintuitive effect of generating new stable states that do not exist in the absence of fluctuations (25). In particular, noise-induced bistability has been reported theoretically (26, 27) and experimentally (2). In those situations, one of the two stable solution branches is usually present irrespective of fluctuations, whereas the second one is purely induced by noise (28). The appearance of such noise-induced branches of solutions requires particular nonlinearities in the underlying equations, and frequently an extrinsic noise source. It is thus of interest to establish mechanisms through which noise-induced stabilization can be caused by noise that is intrinsic to the biochemical reactions that comprise biological systems. Furthermore, because of the limited number of examples of noise-induced stabilization, it is unclear if and what different mechanisms can support this counterintuitive phenomenon.

The address the questions raised above, we have investigated a prototypical two-component activator–repressor genetic circuit as a model system (Fig. 1*A*). This circuit comprises a promoter (P_a) that expresses a transcription factor (A) that can activate both its own promoter (P_a) and the promoter of a repressor (P_r). The repressor protein (R) can inhibit the activity of the transcription factor (A) by targeting it for degradation. The autoregulation of the activator forms a positive feedback loop, whereas the activation of the repressor (R) and the consecutive inhibition of the activator molecule (A) by the repressor (R) establish a net negative feedback loop. Expression of activator and repressor transcription factors is thus synchronized where A and R can both be either high or low. Thus, this system constitutes a simple genetic circuit with interacting positive and negative feedback loops.

Natural genetic circuits that are composed of such interacting positive and negative feedback loops typically support various nonlinear dynamic behaviors (29). In particular, this circuit topology is common among genetic oscillators, such as cell cycle and circadian clocks (30–35). Additionally, transient cellular processes such as cell membrane polarization in neurons (36), yeast (37), and differentiation in bacteria (17, 18, 20) are also controlled by genetic circuits that are similar in architecture. Therefore, understanding how noise influences the dynamics of genetic circuits with this shared topology will be of general relevance to a wide range of cellular processes. Furthermore, a mechanistic understanding of the effects of noise on this simple circuit could guide the engineering of synthetic circuits with nonlinear dynamical behavior.

This investigation of the prototypical activator–inhibitor circuit described above shows that intrinsic noise is able to effectively stabilize an unstable state via a mechanism distinct and much simpler than those proposed to date. Below, we present results that demonstrate that intrinsic noise stabilizes an unstable fixed point that already exists deterministically. Specifically, when an unstable spiral point coexists with a second stable state from which it is separated by a saddle point, the phase-space topology is such that stochastic fluctuations are able to induce stochastic oscillations (38) around the unstable spiral. These oscillations in turn lead to increased dwell times in the region of space around the unstable fixed point, and therefore to its effective stabilization. We remark that, in our case, the effect is caused by standard intrinsic noise and does not require an external noise source.

Interestingly, this stabilization mechanism based on noise-induced oscillations around the unstable state also restricts the time window during which switching from the unstable high-expression

Author contributions: J.G.-O. and G.M.S. designed research; M.T. and J.G.-O. performed research; M.T., J.G.-O., and G.M.S. analyzed data; and J.G.-O. and G.M.S. wrote the paper.

The authors declare no conflict of interest.

This article is a PNAS Direct Submission.

Freely available online through the PNAS open access option.

§To whom correspondence should be addressed. E-mail: gurol.suel@utsouthwestern.edu.

www.pnas.org/cgi/doi/10.1073/pnas.0806349105

Parallel pathways of repression and antirepression governing the transition to stationary phase in *Bacillus subtilis*

Allison V. Banse, Arnaud Chastanet, Lilah Rahn-Lee, Errett C. Hobbs*, and Richard Losick†

Department of Molecular and Cellular Biology, Harvard University, Cambridge, MA 02138

Edited by Sankar Adhya, National Institutes of Health, Bethesda, MD, and approved August 27, 2008 (received for review May 29, 2008)

The AbrB protein of the spore-forming bacterium *Bacillus subtilis* is a repressor of numerous genes that are switched on during the transition from the exponential to the stationary phase of growth. The gene for AbrB is under the negative control of the master regulator for entry into sporulation, Spo0A~P. It has generally been assumed that derepression of genes under the negative control of AbrB is achieved by Spo0A~P-mediated repression of *abrB* followed by rapid degradation of the AbrB protein. Here, we report that AbrB levels do decrease during the transition to stationary phase, but that this decrease is not the entire basis by which AbrB-controlled genes are derepressed. Instead, AbrB is inactivated by the product of a uncharacterized gene, *abbA* (formerly *ykzF*), whose transcription is switched on by Spo0A~P. The *abbA* gene encodes an antirepressor that binds to AbrB and prevents it from binding to DNA. Combining our results with previous findings, we conclude that Spo0A~P sets in motion two parallel pathways of repression and antirepression to trigger the expression of diverse categories of genes during the transition to stationary phase.

sporulation | transcription

Bacteria ordinarily spend a relatively brief period of their existence in the exponential phase of growth (1–3). Nutrients become limiting, or other adverse environmental changes take place as cells reach a high population density, causing growth to slow and the bacteria to enter stationary phase. Coping with the transition to stationary phase involves dramatic changes in gene expression in which suites of genes are switched on that enable the cells to adapt to unfavorable circumstances. These changes are governed by signal transduction pathways that sense the onset of adverse circumstances and respond by activating (or inactivating) global regulatory proteins. One such global regulator is the general stress response transcription factor σ^S, which helps govern the transition to stationary phase in *Escherichia coli* (4, 5). In the spore-forming bacterium *Bacillus subtilis*, the subject of this investigation, the transition to stationary phase is principally governed by five regulatory proteins, CodY (6), σ^B (7, 8), σ^H (9), Spo0A~P (10), and AbrB (11).

How CodY helps to govern the transition to stationary phase is well understood. Its activity as a repressor depends on either of two cofactors, GTP or a branched chain amino acid (12, 13). In the absence of either ligand, CodY's ability to bind DNA is impaired. Thus, because GTP or branched chain amino acid levels drop during nutrient limitation, repression is relieved and genes under the control of CodY are derepressed. Our understanding of how σ^B-, σ^H-, and Spo0A-controlled gene expression is coupled to the exit from the exponential phase of growth is less complete. The σ^B factor, for example, is activated by convergent pathways that sense, in an as yet undefined way, the lack of certain nutrients and the presence of certain kinds of physical-chemical signals (14). Spo0A, a member of the response regulator family of phosphoproteins, is activated by phosphorylation in response to nutrient limitation via a multicomponent phosphorelay (15). The phosphorelay is initiated by several kinases that are thought to recognize intra- or extracellular signals. When phosphorylated, Spo0A~P acts as an activator or repressor of ≈120 genes under its direct control, including genes required for sporulation (16). However, how phosphorelay-mediated phosphorylation of Spo0A is coupled to a drop in nutrient availability has not been elucidated.

The fifth transcriptional control protein, the "transition-state regulator" AbrB and the focus of this report, has been of interest for almost 40 years (17–19). Yet little is known about the mechanisms that govern the derepression of AbrB-controlled genes at the end of the exponential phase of growth. The gene for AbrB was discovered because of the observation that mutations at the *abrB* locus suppressed some of the phenotypes characteristic of *spo0A* and other mutants blocked in the initiation of sporulation. However, how AbrB acted was mysterious for many years (20). An important clue came from studies of two promoters that depended on Spo0A~P for their activation (21, 22). In both cases, an *abrB* mutation was found to bypass the dependence on *spo0A*, and in one case, it resulted in constitutive transcription. These findings indicated that AbrB is likely a repressor that is present in vegetatively growing cells and is inactivated or eliminated by the action of Spo0A at the end of the exponential phase of growth. Indeed, subsequent biochemical work confirmed that AbrB is a DNA-binding protein that acts by repressing target genes (23, 24). The further demonstration that Spo0A~P directly represses *abrB* (25) led to the view that derepression of genes under AbrB control is mediated by a Spo0A~P-imposed block in *abrB* transcription combined with rapid depletion of AbrB protein by degradation (24, 26, 27).

As we report here, AbrB levels do decrease as cells transition from exponential growth to stationary phase, but this drop in AbrB levels is not the sole basis for the derepression of genes under its control. Instead, AbrB is inactivated by the product of a previously uncharacterized gene, *ykzF* (for which we introduce the name *abbA* for *a*ntirepressor of *abrB A*) that is directly switched on by Spo0A~P (16, 28). We show that *abbA* encodes an AbrB-binding protein that forms a complex with the repressor and prevents it from adhering to DNA. Thus, the derepression of some or all genes under the negative control of AbrB involves the Spo0A~P-induced synthesis of an antirepressor. A parallel thereby emerges between AbrB and the SinR repressor of *B.*

Author contributions: A.V.B., L.R.-L., E.C.H., and R.L. designed research; A.V.B., A.C., L.R.-L., and E.C.H. performed research; A.V.B., A.C., L.R.-L., and R.L. analyzed data; and A.V.B. and R.L. wrote the paper.

The authors declare no conflict of interest.

This article is a PNAS Direct Submission.

*Present address: Cell Biology and Metabolism Program, Eunice Kennedy Shriver National Institute of Child Health and Human Development, Bethesda, MD 20892.

†To whom correspondence should be addressed. E-mail: losick@mcb.harvard.edu.

This article contains supporting information online at www.pnas.org/cgi/content/full/0805203105/DCSupplemental.

Exploring RNA transcription and turnover *in vivo* by using click chemistry

Cindy Y. Jao and Adrian Salic*

Department of Cell Biology, Harvard Medical School, 240 Longwood Avenue, Boston, MA 02115

Communicated by Howard Green, Harvard Medical School, Boston, MA, August 28, 2008 (received for review June 18, 2008)

We describe a chemical method to detect RNA synthesis in cells, based on the biosynthetic incorporation of the uridine analog 5-ethynyluridine (EU) into newly transcribed RNA, on average once every 35 uridine residues in total RNA. EU-labeled cellular RNA is detected quickly and with high sensitivity by using a copper (I)-catalyzed cycloaddition reaction (often referred to as "click" chemistry) with fluorescent azides, followed by microscopic imaging. We demonstrate the use of this method in cultured cells, in which we examine the turnover of bulk RNA after EU pulses of varying lengths. We also use EU to assay transcription rates of various tissues in whole animals, both on sections and by whole-mount staining. We find that total transcription rates vary greatly among different tissues and among different cell types within organs.

5-ethynyluridine | microscopy | azide | alkyne | fluorescence

Two methods have been used to measure rates of total transcription in cells. The first method relies on labeling RNA with radioactive nucleosides followed by tissue autoradiography (1). Autoradiography is very slow, requiring exposure times of weeks to months (1); working with radioactivity is also cumbersome and the spatial resolution of the microscopic images obtained is poor.

The second method measures incorporation into RNA of 5-bromouridine (BrU), delivered to cells either as 5-bromouridine triphosphate (BrUTP) or as BrU. Because cells are impermeable to BrUTP, they must be microinjected with it (2, 3), permeabilized in the presence of BrUTP (4), transfected with BrUTP liposomes (5), scratch labeled (6), or loaded with BrUTP by osmotic shock (7). Aside from the high cost of BrUTP, the methods are labor intensive and not applicable to all cell types or to whole-animal studies. BrU is taken up by cells and incorporated into the pool of nucleotide phosphates by means of the ribonucleoside salvage pathway. Cells are then fixed and BrU incorporation into RNA is detected by immunostaining (8). One of the main disadvantages of BrU detection is that, being an antibody-based method, staining of tissues is limited by antibody diffusion into the specimen. Thus, tissues have to be sectioned and whole-mount examination of RNA synthesis in tissues and organs is practically very limited.

We recently described a chemical method to assay DNA synthesis *in vivo* by using 5-ethynyl-2′-deoxyuridine (EdU), a thymidine analog that incorporates efficiently into DNA (9). EdU can be detected rapidly and with great sensitivity with fluorescent azides by means of a Sharpless–Meldal copper (I)-catalyzed Huisgen cycloaddition reaction (10, 11), a highly efficient and selective reaction often referred to as a "click" reaction. We have now extended this methodology to devise a chemical method to assay RNA synthesis *in vivo*.

We show that 5-ethynyluridine (EU) is incorporated into RNA transcripts generated by RNA polymerases I, II, and III in cells. EU-labeled cellular RNA can be detected quickly and with high sensitivity with fluorescent azides. Detection of EU is much faster than an anti-BrU immunostain and allows whole-mount staining of large organ and tissue fragments. Conveniently, EU does not significantly label cellular DNA, thus making it a specific transcriptional label. We demonstrate the use of EU in assaying the turnover of bulk transcripts in cultured cells. Last, we use EU in whole animals to reveal bulk transcriptional patterns in several organs and tissues.

Due to its ease and sensitivity, we anticipate the EU labeling method [particularly through labeling individual RNAs *in vitro* with 5-ethynyluridine triphosphate (EUTP)] will facilitate high-resolution microscopic analysis of RNA synthesis, transport, localization, and turnover *in vivo*.

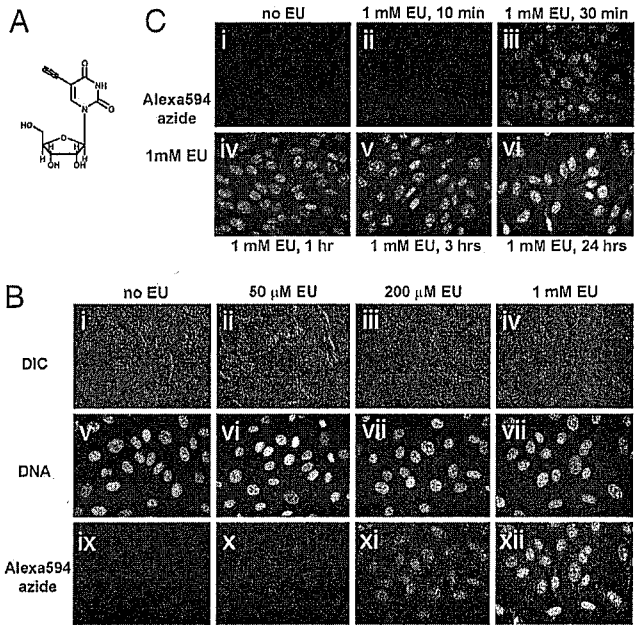

Fig. 1. Imaging cellular transcription by using EU. (*A*) Structure of the uridine analog EU, a biosynthetic RNA label. (*B*) EU incorporation into RNA in NIH 3T3 cells. Cells were grown without EU (*i*, *v*, and *ix*), with 50 μM EU (*ii*, *vi*, and *x*), 200 μM EU (*iii*, *vii*, and *xi*), or 1 mM EU (*iv*, *viii*, and *xii*) for 20 h. The cells were fixed and reacted with 10 μM Alexa594-azide. EU-labeled cells show strong nuclear and weaker cytoplasmic staining, proportional to the added EU concentration. Note the intense staining of nucleoli. All cells incorporate EU, although some cell-to-cell variability is observed. (*C*) Rapid uptake and incorporation of EU by cells. NIH 3T3 cells were incubated with 1 mM EU for varying amounts of time, followed by fixation and EU detection. Strong nuclear staining is visible after 30 min (*iii*), although even after 10 min (*ii*), a signal above background is observed at longer exposure times (data not shown). EU staining intensity increases quickly in the first 3 h (*iv* and *v*) and then more slowly up to 24 h (*vi*).

Author contributions: C.Y.J. and A.S. designed research; C.Y.J. and A.S. performed research; C.Y.J. and A.S. analyzed data; and A.S. wrote the paper.

The authors declare no conflict of interest.

*To whom correspondence should be addressed. E-mail: asalic@hms.harvard.edu.

Vol 455|25 September 2008|doi:10.1038/nature07292

ARTICLES

Frequency-modulated nuclear localization bursts coordinate gene regulation

Long Cai[1]*, Chiraj K. Dalal[1]* & Michael B. Elowitz[1]

In yeast, the transcription factor Crz1 is dephosphorylated and translocates into the nucleus in response to extracellular calcium. Here we show, using time-lapse microscopy, that Crz1 exhibits short bursts of nuclear localization (typically lasting 2 min) that occur stochastically in individual cells and propagate to the expression of downstream genes. Strikingly, calcium concentration controls the frequency, but not the duration, of localization bursts. Using an analytic model, we also show that this frequency modulation of bursts ensures proportional expression of multiple target genes across a wide dynamic range of expression levels, independent of promoter characteristics. We experimentally confirm this theory with natural and synthetic Crz1 target promoters. Another stress-response transcription factor, Msn2, exhibits similar, but largely uncorrelated, localization bursts under calcium stress suggesting that frequency-modulation regulation of localization bursts may be a general control strategy used by the cell to coordinate multi-gene responses to external signals.

Cells sense extracellular signals and respond by regulating the expression of target genes[1–3]. This process requires two stages of information processing. First, cells encode extracellular signals internally, in the states and localization of transcription factors. Second, transcription factors activate the expression of downstream genes that will implement cellular responses[1–3]. Although many signal transduction systems have been studied extensively, it often remains unclear how signals are encoded dynamically in transcription factor activities at the single-cell level. In addition, cellular responses often involve many proteins acting together, rather than individually. However, in general it is not known how the expression levels of target genes are coordinated, allowing them to be regulated together, despite diverse promoter architectures[3]. Here we investigate how signal encoding and protein coordination are achieved in individual cells.

We examined the calcium stress response pathway in *Saccharomyces cerevisiae*, or budding yeast. Cellular responses to extracellular calcium are mediated by Crz1, the calcineurin-responsive zinc finger transcription factor[4]. The activity of Crz1 is modulated by phosphorylation and dephosphorylation[4], resulting in changes in the nuclear localization of Crz1 protein (Fig. 1a), rather than changes in its abundance (Supplementary Fig. 1). To understand how Crz1 phosphorylation dynamics respond to calcium and regulate the more than 100 different targets necessary for calcium adaptation[5], we acquired time-lapse movies of Crz1 localization dynamics, using a strain in which the Crz1 protein was tagged with green fluorescent protein (GFP)[6]. In each movie, we tracked the response of Crz1 localization in individual cells to step changes in extracellular calcium concentration. We found that Crz1 dynamics connect the encoding of signals and the coordination of target gene expression.

Frequency modulated bursts of nuclear localization

In the absence of calcium, Crz1 was cytoplasmic in all cells (Supplementary Movie 1). Upon the addition of calcium, individual cells exhibited a rapid, synchronized burst of Crz1 nuclear localization, similar to behaviour observed with the yeast osmosensor Hog1 (refs 7, 8). However, unlike Hog1, this initial burst was followed by sporadic unsynchronized localization bursts, typically lasting about 2 min (Fig. 1b–d) and persisting throughout the course of the movie (up to 10 h, see Supplementary Movie 1). Moreover, these single-cell Crz1 dynamics are consistent with microarray studies performed on cell populations[5]: after a step change in calcium, an initial overshoot in messenger RNA levels of Crz1 target genes results from the initial synchronous burst of Crz1, whereas the subsequent elevated average expression levels are due to sustained unsynchronized bursts in individual cells (Fig. 1c–e).

We next addressed how the amount of calcium affects the dynamics of nuclear localization. We observed that the fraction of cells with nuclear-localized Crz1 increased with calcium concentration. Because Crz1 localizes in bursts, this calcium dependence could in principle result from increases in burst frequency or duration. Strikingly, analysis of movies revealed that only the burst frequency increased (Fig. 2a), whereas the distribution of burst durations remained constant at all calcium concentrations (Fig. 2b). This distribution was consistent with two rate-limiting stochastic steps, each with a timescale of about 70 s (Fig. 2b). Thus, cells use stereotyped Crz1 localization bursts in a frequency-modulated fashion to encode and respond to extracellular calcium. This contrasts with amplitude-modulation control, in which the fraction of Crz1 molecules found in the nucleus would change with calcium, but remain constant over time.

Movies also revealed two modes of nuclear localization bursts: isolated individual bursts and clusters of bursts, analogous to spike trains in neurons (Fig. 1c, d). At calcium concentrations less than 100 mM, only isolated bursts were observed and the averaged autocorrelation function of the localization trajectories from individual cells was well fitted by a single exponential. However, as clustered bursts emerged at calcium concentrations greater than 100 mM (Fig. 1c, d), the averaged autocorrelation function was better fit by a sum of two exponentials, whose timescales matched the typical durations of isolated bursts and burst clusters, respectively (Fig. 2d). Higher levels of calcium led to an increasing proportion of bursts occurring in clusters (Fig. 2d inset). Eventually, at the highest calcium levels, Crz1 nuclear localization trajectories appeared more similar to sustained oscillations[9] than to the isolated stochastic bursts seen at lower calcium concentrations.

[1]Howard Hughes Medical Institute, Division of Biology and Department of Applied Physics, California Institute of Technology, M/C 114-96, Pasadena, California 91125, USA.
*These authors contributed equally to this work.

Vol 454|28 August 2008|doi:10.1038/nature07195

ARTICLES

Misfolded proteins partition between two distinct quality control compartments

Daniel Kaganovich[1], Ron Kopito[1] & Judith Frydman[1]

The accumulation of misfolded proteins in intracellular amyloid inclusions, typical of many neurodegenerative disorders including Huntington's and prion disease, is thought to occur after failure of the cellular protein quality control mechanisms. Here we examine the formation of misfolded protein inclusions in the eukaryotic cytosol of yeast and mammalian cell culture models. We identify two intracellular compartments for the sequestration of misfolded cytosolic proteins. Partition of quality control substrates to either compartment seems to depend on their ubiquitination status and aggregation state. Soluble ubiquitinated misfolded proteins accumulate in a juxtanuclear compartment where proteasomes are concentrated. In contrast, terminally aggregated proteins are sequestered in a perivacuolar inclusion. Notably, disease-associated Huntingtin and prion proteins are preferentially directed to the perivacuolar compartment. Enhancing ubiquitination of a prion protein suffices to promote its delivery to the juxtanuclear inclusion. Our findings provide a framework for understanding the preferential accumulation of amyloidogenic proteins in inclusions linked to human disease.

The strong correlation between the accumulation of aggregated proteins in amyloid inclusions and the onset of several neurodegenerative diseases calls for a better understanding of the mechanisms and functions of inclusion formation. Research indicating that soluble aggregation intermediates have a toxic 'gain of function' activity suggests that regulated formation of protein inclusions serves cytoprotective functions, such as sequestering misfolded species[1–7], and it may also facilitate their clearance[8–12]. It is unknown whether inclusions contain only terminally aggregated proteins or whether they also sequester soluble misfolded conformations[13]. Intriguingly, although all proteins can form amyloid-like inclusions after misfolding[1,14], only a handful of proteins cause amyloidosis and disease[2]. In principle, these amyloidogenic disease-related proteins may interact differently with the cellular quality control machinery. Thus, characterization of the pathways leading to inclusion formation is critical for understanding the basis of protein conformation disorders.

Cellular inclusions form in an organized process that seems to be conserved from yeast to mammalian cells[2,8,15]. Distinct inclusions with specific characteristics have been observed[13,16–19], including insoluble perinuclear inclusions (called aggresomes) that co-localize with the microtubule organizing centre[20], perinuclear inclusions containing soluble endoplasmic reticulum associated protein degradation (ERAD) substrates[18,21], and inclusions co-localizing with autophagic markers[9,10]. It is unclear whether all these observations pertain to the same compartment or what underlies the distinct solubility and long-term fates observed for different quality control substrates in these inclusions.

Unlike amyloidogenic proteins, little is known about the fate of 'normal' misfolded cytosolic globular proteins[22]. Protein misfolding can arise as a consequence of stress-induced denaturation, destabilizing missense mutations or lack of oligomeric assembly partners. To examine how cytosolic quality control proceeds in these different scenarios, we chose a panel of model substrates corresponding to each case (Fig. 1) and compared their fate to that of model amyloidogenic proteins (Fig. 2). Our findings show that the quality control machinery partitions misfolded proteins, on the basis of their ubiquitination state and solubility, among two distinct quality control compartments. Interestingly, amyloidogenic proteins are preferentially sorted to only one of these compartments. These distinct quality control compartments may represent two cellular strategies for the sequestration of aggregation prone, potentially toxic polypeptides.

Two compartments for misfolded cytosolic proteins

To determine the fate of cytosolic misfolded substrates, we initially followed a destabilized Ubc9 variant that misfolds above 30 °C (refs 23, 24; Fig. 1a). Ubc9^{ts}, fused to green fluorescent protein (GFP) to facilitate detection (GFP–Ubc9^{ts}), was expressed under the control of a galactose-regulated promoter. Glucose addition repressed expression, allowing us to follow the fate of GFP–Ubc9^{ts} from the earliest stages of protein misfolding after shift to 37 °C (Fig. 1a). At permissive temperatures, GFP–Ubc9^{ts} was native and diffuse, similar to wild-type GFP–Ubc9 (Fig. 1b, 0 min, compare with wild type panel 120 min). GFP–Ubc9^{ts} misfolding led to degradation by the ubiquitin–proteasome pathway, as reported for untagged Ubc9^{ts} (Fig. 1b, compare 5 min and 60 min; and Fig. 1d, left panel)[23,24]. During degradation we observed transient accumulation of Ubc9^{ts} in distinct cytosolic puncta and inclusions that were eventually cleared (for example, Fig. 1b, 30 min and Fig. 1c). Most cells contained a juxtanuclear inclusion as well as smaller puncta throughout the cytosol, whereas some cells contained only the juxtanuclear inclusion (Fig. 1b, c). Impairment of proteasome-mediated degradation either in *cim3-1* cells or by treatment with the proteasome inhibitor MG132 stabilized GFP–Ubc9^{ts} and led to its reproducible accumulation in two distinct inclusions in virtually every cell (Fig. 1b, 60 min and 120 min and Supplementary Fig. 1a). At early time points after misfolding in proteasome-defective cells, GFP–Ubc9^{ts} accumulated in structures resembling those observed during degradation in control cells (Fig 1b, compare 15 min and 30 min). Quantification indicated that the juxtanuclear inclusion formed first, closely followed by cytosolic puncta (Fig. 1c). However, at later incubation times at 37 °C the juxtanuclear inclusion remained, but the puncta were no longer observed. Instead, a second large perivacuolar inclusion was now formed at the periphery of the cell (Fig. 1b, c). Once formed, both

[1]Department of Biology and BioX Program, Stanford University, Stanford, California 94305, USA.

LETTERS

Self-destructive cooperation mediated by phenotypic noise

Martin Ackermann[1], Bärbel Stecher[2], Nikki E. Freed[1], Pascal Songhet[2], Wolf-Dietrich Hardt[2] & Michael Doebeli[3]

In many biological examples of cooperation, individuals that cooperate cannot benefit from the resulting public good. This is especially clear in cases of self-destructive cooperation, where individuals die when helping others. If self-destructive cooperation is genetically encoded, these genes can only be maintained if they are expressed by just a fraction of their carriers, whereas the other fraction benefits from the public good. One mechanism that can mediate this differentiation into two phenotypically different sub-populations is phenotypic noise[1,2]. Here we show that noisy expression of self-destructive cooperation can evolve if individuals that have a higher probability for self-destruction have, on average, access to larger public goods. This situation, which we refer to as assortment, can arise if the environment is spatially structured. These results provide a new perspective on the significance of phenotypic noise in bacterial pathogenesis: it might promote the formation of cooperative sub-populations that die while preparing the ground for a successful infection. We show experimentally that this model captures essential features of *Salmonella typhimurium* pathogenesis. We conclude that noisily expressed self-destructive cooperative actions can evolve under conditions of assortment, that self-destructive cooperation is a plausible biological function of phenotypic noise, and that self-destructive cooperation mediated by phenotypic noise could be important in bacterial pathogenesis.

Recent experimental work demonstrated that genetically identical organisms living in the same environment show surprisingly high levels of variation in phenotypic traits[1,2], and sometimes even switch between distinct phenotypic states[3]. Stochastic cellular processes are one source of such phenotypic noise. The level of phenotypic noise is subject to mutational change, and can thus evolve. This raises the question whether natural selection always acts towards minimizing phenotypic noise, or whether there are cases in which genotypes that encode variable phenotypes are favoured by selection. In the existing theory[4–6], the most prominent adaptive explanation for phenotypic noise is bet-hedging[5], according to which the stochastic expression of alternative phenotypes allows a genotype to survive changes in external conditions and thus to persist in fluctuating environments.

Here we focus on a fundamentally different adaptive explanation for phenotypic noise: self-destructive cooperation. In this scenario, the individuals that survive and form a successful lineage all express the same phenotype. Individuals that express an alternative phenotype do exist, but they do not contribute to future generations; instead, they die while contributing to a public good that benefits others. There are many examples of cooperative acts that prevent reproduction or survival of the actor, ranging from non-reproductive workers in mammals and insects to unicellular bacteria that lyse when releasing chemical substances that benefit others. Importantly, genotypes that have the propensity to express self-destructive cooperation can only persist if the expression is limited to a fraction of the individuals carrying the genotype, whereas another fraction does not express the cooperative behaviour and benefits from the public good produced. Sometimes, this differentiation into two fractions is mediated by signals. In other examples, notably in microorganisms, there seems to be no signal. In these cases, phenotypic noise could promote the differentiation required for self-destructive cooperation to persist.

We investigated the evolutionary dynamics of a self-destructive cooperative act that contributes to the generation of a public good and that is expressed in a stochastic manner. In general, cooperation can evolve if cooperative individuals benefit from cooperative acts of others more often than non-cooperative individuals[7]—a situation referred to as assortment. We used a simple model to quantify the level of assortment as a function of the external conditions, and to calculate how selection on the probability to express self-destructive cooperation depends on the level of assortment, as well as on the amount of public good generated by cooperative acts.

The model is based on the public goods game and assumes that there are two strategies: cooperate (C) and defect (D). C sacrifices itself with probability q, and only if it sacrifices itself, it contributes an amount b to the public good. The decision between sacrificing and not sacrificing is a chance outcome resulting from phenotypic bistability; every cooperator makes this decision independently of the environment or of the decisions of other individuals. D never contributes to the public good. The game is played in interaction groups of N players. In general, if there are k cooperators among the N members of an interaction group, the total amount of the public good produced in that group is kqb. The total amount of the public good is available to each surviving player in the interaction group (an alternative scenario where the public good is divided among the surviving players gives very similar results). We assume that, in addition to the public good, all players also receive a non-zero baseline payoff w.

Consider first the payoff to a focal C player in a given interaction group. Because the focal C is one of the k cooperators, its social environment consists of $k-1$ cooperators and $N-k$ defectors. The focal C gets no payoff from the defectors, but if it survives it receives the benefit b with a probability q from each of the other $k-1$ cooperators, as well as the baseline payoff w. The probability that the focal C does not sacrifice itself is $1-q$, and hence the expected payoff to C in the given interaction group is:

$$p_C(N,k) = (1-q)((k-1)qb+w) \qquad (1)$$

The social environment of a focal D in the given interaction group consists of k cooperators and $N-k-1$ defectors, and its expected payoff is:

[1]Institute of Integrative Biology, ETH Zurich, 8092 Zürich, Switzerland. [2]Institute of Microbiology, ETH Zurich, 8093 Zürich, Switzerland. [3]Department of Zoology and Department of Mathematics, University of British Columbia, Vancouver BC V6T 1Z4, Canada.

LETTERS

Correlation between nanosecond X-ray flashes and stick–slip friction in peeling tape

Carlos G. Camara[1]*, Juan V. Escobar[1]*, Jonathan R. Hird[1] & Seth J. Putterman[1]

Relative motion between two contacting surfaces can produce visible light, called triboluminescence[1]. This concentration of diffuse mechanical energy into electromagnetic radiation has previously been observed to extend even to X-ray energies[2]. Here we report that peeling common adhesive tape in a moderate vacuum produces radio and visible emission[3,4], along with nanosecond, 100-mW X-ray pulses that are correlated with stick–slip peeling events. For the observed 15-keV peak in X-ray energy, various models[5,6] give a competing picture of the discharge process, with the length of the gap between the separating faces of the tape being 30 or 300 μm at the moment of emission. The intensity of X-ray triboluminescence allowed us to use it as a source for X-ray imaging. The limits on energies and flash widths that can be achieved are beyond current theories of tribology.

When a continuous medium is driven far from equilibrium, nonlinear processes can lead to strong concentrations in the energy density. Sonoluminescence[7] provides an example in which acoustic energy concentrates by 12 orders of magnitude to generate subnanosecond flashes of ultraviolet radiation. Charge separation at contacting surfaces[8,9] is another example of a process that funnels diffuse mechanical energy into high-energy emission. Lightning[10], for instance, has been shown to generate X-rays with energies of more than 10 keV (ref. 11). Although triboelectrification is important in many natural and industrial processes, its physical explanation is still debated[10,12].

By peeling pressure-sensitive adhesive tape one realizes an everyday example of tribocharging and triboluminescence[1]: the emission of visible light. Tape provides a particularly interesting example of these phenomena because it has been claimed that the fundamental energy that holds tape to a surface is provided by the van der Waals interaction[13]. This energy—the weakest in chemistry—is almost 100-fold smaller than the energy required for generating a visible photon, yet, as demonstrated in 1939 (ref. 3), light emission from peeling tape can be seen with the unaided eye. That even more energetic processes were at play had already been suggested in 1930 (ref. 14); it was observed that when mica is split under vacuum "the glass of the vessel fluoresces like an X-ray bulb". This insight led to the discovery in 1953 (ref. 2) that peeling tape is a source of X-rays. The simultaneous emission of visible and X-ray photons from peeling tape is shown in Fig. 1a, in which the blue glow is due to a scintillator responsive to X-ray energies and the red patch near the peel point is neon-enhanced triboluminescence[3]. Figure 1b shows that when the vacuum pressure is 10^{-3} torr the high-energy emission is so strong that the photo is illuminated entirely with scintillations.

Motivated by these photos, we interpret triboluminescence[1], a phenomenon known for centuries, as being part of an energy-density-focusing process that can extend four orders of magnitude beyond visible light to X-ray photons. To learn about the processes occurring in peeling tape, we employed efficient high-speed X-ray detection equipment. Our measurements indicated that the scintillations in

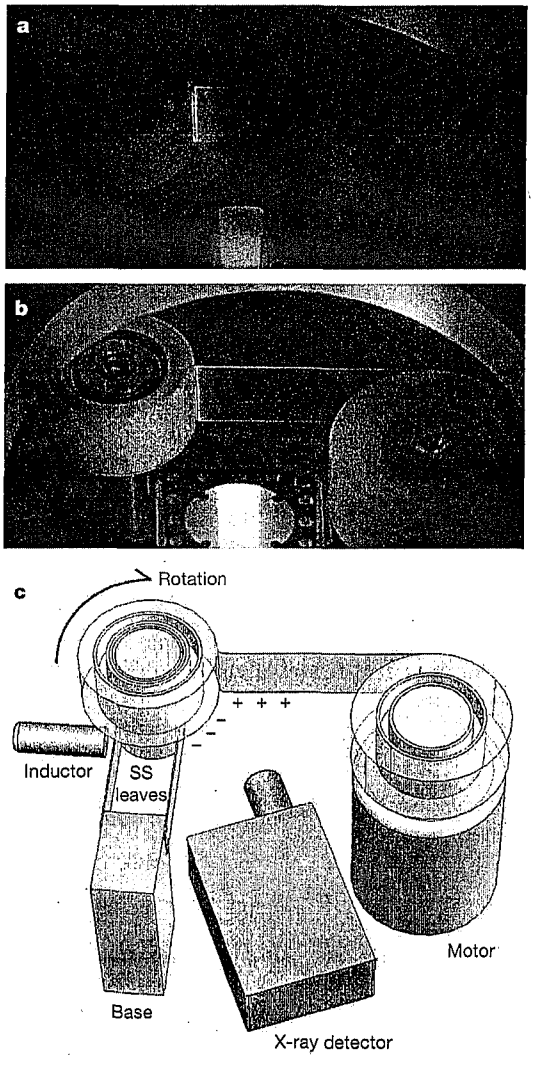

Figure 1 | Apparatus for studying high-energy emission from peeling tape. **a**, Photograph of the simultaneous emission of triboluminescence (red line) and scintillations of a phosphor screen sensitive to electron impacts with energies in excess of 500 eV (under neon at a pressure of 150 mtorr). **b**, Photograph of the apparatus (under a pressure of 10^{-3} torr) illuminated entirely by scintillations. **c**, Diagram of the apparatus used to measure peeling force; SS, spring steel (Methods).

[1]Department of Physics and Astronomy, University of California, Los Angeles, Los Angeles, California 90095, USA.
*These authors contributed equally to this work.

A genetic timer through noise-induced stabilization of an unstable state

Marc Turcotte*, Jordi Garcia-Ojalvo†, and Gürol M. Süel*‡§

*Department of Pharmacology, University of Texas Southwestern Medical Center, Dallas, TX 753903; †Departament de Física i Enginyeria Nuclear, Universitat Politècnica de Catalunya, Colom 11, E-08222 Terrassa, Spain; and ‡Green Center for Systems Biology, University of Texas Southwestern Medical Center, Dallas, TX 75390

Edited by José N. Onuchic, University of California at San Diego, La Jolla, CA, and approved August 27, 2008 (received for review July 1, 2008)

Stochastic fluctuations affect the dynamics of biological systems. Typically, such noise causes perturbations that can permit genetic circuits to escape stable states, triggering, for example, phenotypic switching. In contrast, studies have shown that noise can surprisingly also generate new states, which exist solely in the presence of fluctuations. In those instances noise is supplied externally to the dynamical system. Here, we present a mechanism in which noise intrinsic to a simple genetic circuit effectively stabilizes a deterministically unstable state. Furthermore, this noise-induced stabilization represents a unique mechanism for a genetic timer. Specifically, we analyzed the effect of noise intrinsic to a prototypical two-component gene-circuit architecture composed of interacting positive and negative feedback loops. Genetic circuits with this topology are common in biology and typically regulate cell cycles and circadian clocks. These systems can undergo a variety of bifurcations in response to parameter changes. Simulations show that near one such bifurcation, noise induces oscillations around an unstable spiral point and thus effectively stabilizes this unstable fixed point. Because of the periodicity of these oscillations, the lifetime of the noise-dependent stabilization exhibits a polymodal distribution with multiple, well defined, and regularly spaced peaks. Therefore, the noise-induced stabilization presented here constitutes a minimal mechanism for a genetic circuit to function as a timer that could be used in the engineering of synthetic circuits.

bifurcation | dynamics | circuit | stochastic | quantized cycle

Stochastic fluctuations in gene expression and protein concentrations are a natural by-product of biochemical reactions in cells. Properties of this biochemical noise within genetic circuits, such as their amplitude, distribution, and propagation, have been extensively characterized (1–9). Additionally, theoretical and experimental studies have established that such noise can induce stochastic switching between distinct and stable phenotypic states (5, 10–23). Noise within genetic circuits is therefore thought to contribute to phenotypic heterogeneity in genetically identical cellular populations. It has also recently been shown experimentally that noise can trigger cellular differentiation in fruit flies and bacteria (14, 17, 18, 24). Together, these studies establish that noise can play an active functional role in cellular processes by effectively destabilizing and thus inducing escape from stable phenotypic states.

Besides its common role in destabilizing stable states, noise can also have the more counterintuitive effect of generating new stable states that do not exist in the absence of fluctuations (25). In particular, noise-induced bistability has been reported theoretically (26, 27) and experimentally (2). In those situations, one of the two stable solution branches is usually present irrespective of fluctuations, whereas the second one is purely induced by noise (28). The appearance of such noise-induced branches of solutions requires particular nonlinearities in the underlying equations, and frequently an extrinsic noise source. It is thus of interest to establish mechanisms through which noise-induced stabilization can be caused by noise that is intrinsic to the biochemical reactions that comprise biological systems. Furthermore, because of the limited number of examples of noise-induced stabilization, it is unclear if and what different mechanisms can support this counterintuitive phenomenon.

The address the questions raised above, we have investigated a prototypical two-component activator–repressor genetic circuit as a model system (Fig. 1*A*). This circuit comprises a promoter (P_a) that expresses a transcription factor (A) that can activate both its own promoter (P_a) and the promoter of a repressor (P_r). The repressor protein (R) can inhibit the activity of the transcription factor (A) by targeting it for degradation. The autoregulation of the activator forms a positive feedback loop, whereas the activation of the repressor (R) and the consecutive inhibition of the activator molecule (A) by the repressor (R) establish a net negative feedback loop. Expression of activator and repressor transcription factors is thus synchronized where A and R can both be either high or low. Thus, this system constitutes a simple genetic circuit with interacting positive and negative feedback loops.

Natural genetic circuits that are composed of such interacting positive and negative feedback loops typically support various nonlinear dynamic behaviors (29). In particular, this circuit topology is common among genetic oscillators, such as cell cycle and circadian clocks (30–35). Additionally, transient cellular processes such as cell membrane polarization in neurons (36), yeast (37), and differentiation in bacteria (17, 18, 20) are also controlled by genetic circuits that are similar in architecture. Therefore, understanding how noise influences the dynamics of genetic circuits with this shared topology will be of general relevance to a wide range of cellular processes. Furthermore, a mechanistic understanding of the effects of noise on this simple circuit could guide the engineering of synthetic circuits with nonlinear dynamical behavior.

This investigation of the prototypical activator–inhibitor circuit described above shows that intrinsic noise is able to effectively stabilize an unstable state via a mechanism distinct and much simpler than those proposed to date. Below, we present results that demonstrate that intrinsic noise stabilizes an unstable fixed point that already exists deterministically. Specifically, when an unstable spiral point coexists with a second stable state from which it is separated by a saddle point, the phase-space topology is such that stochastic fluctuations are able to induce stochastic oscillations (38) around the unstable spiral. These oscillations in turn lead to increased dwell times in the region of space around the unstable fixed point, and therefore to its effective stabilization. We remark that, in our case, the effect is caused by standard intrinsic noise and does not require an external noise source.

Interestingly, this stabilization mechanism based on noise-induced oscillations around the unstable state also restricts the time window during which switching from the unstable high-expression

Author contributions: J.G.-O. and G.M.S. designed research; M.T. and J.G.-O. performed research; M.T., J.G.-O., and G.M.S. analyzed data; and J.G.-O. and G.M.S. wrote the paper.

The authors declare no conflict of interest.

This article is a PNAS Direct Submission.

Freely available online through the PNAS open access option.

§To whom correspondence should be addressed. E-mail: gurol.suel@utsouthwestern.edu.

27. M. C. Saraf, A. R. Horswill, S. J. Benkovic, C. D. Maranas, *Proc. Natl. Acad. Sci. U.S.A.* **101**, 4142 (2004).
28. J. M. Christie, M. Salomon, K. Nozue, M. Wada, W. R. Briggs, *Proc. Natl. Acad. Sci. U.S.A.* **96**, 8779 (1999).
29. M. Salomon, J. M. Christie, E. Knieb, U. Lempert, W. R. Briggs, *Biochemistry* **39**, 9401 (2000).
30. J. M. Christie, T. E. Swartz, R. A. Bogomolni, W. R. Briggs, *Plant J.* **32**, 205 (2002).
31. S. M. Harper, J. M. Christie, K. H. Gardner, *Biochemistry* **43**, 16184 (2004).
32. X. Yao, M. K. Rosen, K. H. Gardner, *Nat. Chem. Biol.* **4**, 491 (2008).
33. C. A. Fierke, K. A. Johnson, S. J. Benkovic, *Biochemistry* **26**, 4085 (1987).
34. J. T. Chen, K. Taira, C. P. Tu, S. J. Benkovic, *Biochemistry* **26**, 4093 (1987).
35. D. M. Epstein, S. J. Benkovic, P. E. Wright, *Biochemistry* **34**, 11037 (1995).
36. J. Kuriyan, D. Eisenberg, *Nature* **450**, 983 (2007).
37. We thank members of the Ranganathan and Benkovic labs for discussions, M. Rosen and K. H. Gardner for discussions and sharing of unpublished data and materials, and J. Wang for solvent accessibility calculations. Supported by the Robert A. Welch foundation (R.R.) and a grant from the Defense Advanced Research Projects Agency (R.R. and S.J.B.).

Supporting Online Material
www.sciencemag.org/cgi/content/full/322/5900/438/DC1
Materials and Methods
Figs. S1 to S8
Tables S1 to S4
References

14 April 2008; accepted 9 September 2008
10.1126/science.1159052

A Stochastic Single-Molecule Event Triggers Phenotype Switching of a Bacterial Cell

Paul J. Choi,* Long Cai,*† Kirsten Frieda,‡ X. Sunney Xie§

By monitoring fluorescently labeled lactose permease with single-molecule sensitivity, we investigated the molecular mechanism of how an *Escherichia coli* cell with the *lac* operon switches from one phenotype to another. At intermediate inducer concentrations, a population of genetically identical cells exhibits two phenotypes: induced cells with highly fluorescent membranes and uninduced cells with a small number of membrane-bound permeases. We found that this basal-level expression results from partial dissociation of the tetrameric lactose repressor from one of its operators on looped DNA. In contrast, infrequent events of complete dissociation of the repressor from DNA result in large bursts of permease expression that trigger induction of the *lac* operon. Hence, a stochastic single-molecule event determines a cell's phenotype.

Genetically identical cells in the same environment can exhibit different phenotypes, and a single cell can switch between distinct phenotypes in a stochastic manner (*1*–*4*). In the classic example of lactose metabolism in *Escherichia coli*, the *lac* genes are fully expressed for every cell in a population under high extracellular concentrations of inducers, such as the lactose analog methyl-β-D-thiogalactoside (TMG). However, at moderate inducer concentrations, the *lac* genes are highly expressed in only a fraction of a population, which may confer a fitness advantage for the entire population (*5*). We studied the molecular mechanism that controls the stochastic phenotype switching of a single cell.

Lactose metabolism is controlled by the *lac* operon (*6*, *7*), which consists of the *lacZ*, *lacY*, and *lacA* genes encoding β-galactosidase, lactose permease, and transacetylase, respectively. Expression of the operon is regulated by a transcription factor, the *lac* repressor (*8*), which dissociates from its specific binding sequences of DNA, the *lac* operators, in the presence of an inducer to allow transcription (Fig. 1A). The production of the permease increases inducer influx (*9*), which results in positive feedback on the permease expression level. Above a certain threshold of permease numbers, a cell will remain in a phenotype that is capable of lactose metabolism, and below this threshold, a cell will remain in a phenotype that is incapable of lactose metabolism (*10*, *11*). The former has high fluorescence from the cell membrane when the permease is labeled with a yellow fluorescent protein (YFP), whereas the latter has low fluorescence. The image in Fig. 1B shows the coexistence of both phenotypes in a cell population at intermediate inducer concentrations, characterized by the bimodal distributions of fluorescence intensity in Fig. 1C.

Although it is known that the bistability in the *lac* operon arises from positive feedback (*12*, *13*), the molecular mechanism underlying the initiation of switching between two phenotypes remains unclear. Novick and Weiner deduced that switching from the uninduced state to the induced state occurs through a single rate-limiting molecular process (*12*) rather than a multistep process. They further hypothesized that the random expression of one molecule of permease was enough to trigger induction. However, this has never been observed experimentally because of insufficient sensitivity.

Our group has previously shown that a single fluorescent protein molecule can be visualized in a living bacterial cell by using the method of detection by localization (*14*–*16*). Because a permease molecule is a membrane protein with slow diffusion, its fluorescence label is highly localized as compared with a fluorescent protein in the cytoplasm, which allows for its detection above the background of cellular autofluorescence. Thus, we generated strain SX700, which possesses intact *lac* promoter elements and expresses a functional LacY-YFP fusion protein (fig. S1) from *lacY*'s native chromosomal position (fig. S2). Figure 1B shows a fluorescence image of SX700 cells that allows us to directly count the number of single LacY-YFP molecules present in a cell.

Figure 1D shows the histogram of permease copy numbers in the uninduced fraction of cells, free from the complication of autofluorescence background in the lower peak of Fig. 1C. Evidently, the uninduced cells have 0 to 10 LacY molecules with significant probability, independent of the inducer concentration. Had one permease been enough to trigger induction, all cells in the uninduced subpopulation would have contained zero LacY molecules. Thus, we conclude that a single copy of LacY is not sufficient to induce switching of the phenotype, and the threshold for induction must be much higher than several molecules per cell.

We then set out to determine the threshold of permease molecules for induction. It is experimentally difficult to capture the rare events of phenotype switching in real time. To overcome this difficulty, we prepared cells covering a broad range of permease copy numbers by first fully inducing the cells and subsequently washing out the inducer. We then allowed the cells to divide for one to six generations, during which the initial permeases were partitioned into daughter cells (*17*). Figure 2A shows fluorescence time traces of the cells, normalized by cell size, upon the reintroduction of 40 μM TMG. Although the fluorescence in cells with low permease numbers continued to decay because of cell division and photobleaching, cells with more than 300 initial permease molecules induced again within 3 hours and showed increased fluorescence. Figure 2B shows the probability of induction as a function of initial permease number, which is well fit by a Hill equation with a Hill coefficient of 4.5 and a threshold of ~375 molecules. The large value of the threshold indicates that hundreds of permease molecules are necessary to switch the phenotype.

If the induction is due to a single rate-limiting event as Novick and Weiner argued, there must be a single large burst of permease expression to reach this high threshold. However, only small

Department of Chemistry and Chemical Biology, Harvard University, Cambridge, MA 02138, USA.

*These authors contributed equally to this work.
†Present address: Division of Biology, California Institute of Technology, Pasadena, CA 91125, USA.
‡Present address: Biophysics Program, Stanford University, Stanford, CA 94305, USA.
§To whom correspondence should be addressed. E-mail: xie@chemistry.harvard.edu

Fig. 4. Determining functional interactions among kinases and substrates in the JNK network. Hierarchical clustering of average dJUN-FRET *Z* scores after inhibition by RNAi of components in the JNK phosphorylation network in unmodified (KP), as well as in backgrounds deficient in *ERK*, *hippo*, *MLK*, or *puc*. Functional interactions are defined by the detection of an epistatic interaction between kinase and substrate (white boxes) or when the average *Z* scores of kinases and substrate dsRNAs across all sensitized screens cluster together with a cluster distance metric (an average of uncentered Pearson correlation coefficients) greater than 0.67 (shaded boxes). For example, whereas typically ERK acts as a JNK suppressor, *ERK* RNAi in *MLK*-deficient background (asterisk) leads to a notable decrease in dJUN-FRET reporter activity, which suggests that the ERK can act upstream of JNK via predicted phosphorylation of MLK and JNKK. Alternatively, GSK3 is predicted to target MLK, JNKK, and Dlg1, but only *Z* scores for GSK3, MLK, or JNKK dsRNAs cluster across screens, which suggests that GSK3-mediated phosphorylation of MLK and JNKK, but not Dlg1, is functionally relevant to JNK signaling.

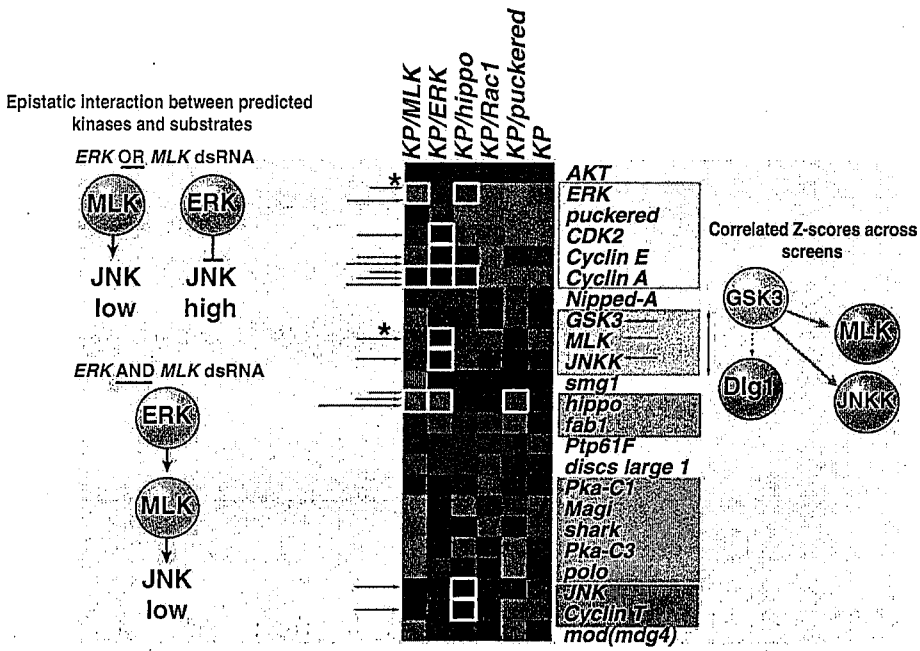

24. L. J. Saucedo, B. A. Edgar, *Nat. Rev. Mol. Cell Biol.* 8, 613 (2007).
25. P. Massimi, D. Gardiol, S. Roberts, L. Banks, *Exp. Cell Res.* 290, 265 (2003).
26. A. Friedman, N. Perrimon, *Nature* 444, 230 (2006).
27. We are deeply indebted to the *Drosophila* RNAi Screening Center and to J. Aach, S. Lee, C. Jørgensen, B. Mathey-Prevot, and B. Bodenmiller. The NetworKIN and NetPhorest algorithms are available at http://networkin.info and http://NetPhorest.info, respectively.

This work is supported by Genome Canada through the Ontario Genomics Institute, the Spanish Ministerio de Ciencia e Innovación (BFU/Consolider 2007), and the European Union (FP6). C.B. is a Fellow of the Leukemia and Lymphoma Society. N.P. is an Investigator of the Howard Hughes Medical Institute.

Supporting Online Material
www.sciencemag.org/cgi/content/full/322/5900/453/DC1
Materials and Methods
SOM Text
Figs. S1 and S2

7 April 2008; accepted 20 August 2008
10.1126/science.1158739

Higher-Order Cellular Information Processing with Synthetic RNA Devices

Maung Nyan Win and Christina D. Smolke*

The engineering of biological systems is anticipated to provide effective solutions to challenges that include energy and food production, environmental quality, and health and medicine. Our ability to transmit information to and from living systems, and to process and act on information inside cells, is critical to advancing the scale and complexity at which we can engineer, manipulate, and probe biological systems. We developed a general approach for assembling RNA devices that can execute higher-order cellular information processing operations from standard components. The engineered devices can function as logic gates (AND, NOR, NAND, or OR gates) and signal filters, and exhibit cooperativity. RNA devices process and transmit molecular inputs to targeted protein outputs, linking computation to gene expression and thus the potential to control cellular function.

Genetically encoded technologies that perform information processing, communication, and control operations are needed to produce new cellular functions from the diverse molecular information encoded in the various properties of small molecules, proteins, and RNA present within biological systems. For example, genetic logic gates that process and translate multiple molecular inputs into prescribed amounts of signaling through new molecular outputs would enable the integration of diverse environmental and intracellular signals to a smaller number of phenotypic responses. Basic operations such as signal filtering, amplification, and restoration would also enable expanded manipulation of molecular information through cellular networks.

Molecular information processing systems have been constructed that perform computation with biological substrates. For example, protein-based systems can perform logic operations to convert molecular inputs to regulated transcriptional events (*1*–*4*). Information processing systems that perform computation on small-molecule and nucleic acid inputs can be constructed from nucleic acid components (*5*–*11*). RNA-based systems can process single inputs to regulated gene expression events (*12*, *13*) and integrate multiple regulatory RNAs for combinatorial gene regulation (*14*, *15*). We sought to combine the rich capability of nucleic acids for performing information processing, transduction, and control operations with the design advantages expected from the relative ease by which RNA structures can be modeled and designed (*16*, *17*).

We proposed a framework for the construction of single input–single output RNA devices (*18*) based on the assembly of three functional components: a sensor component, made of an RNA aptamer (*19*); an actuator component, made of a hammerhead ribozyme (*20*); and a transmitter component, made of a sequence that couples the sensor and actuator components. The resulting devices distribute between two primary conformations: one in which the input cannot bind the sensor, and the other in which the input can bind the sensor as a result of competitive hybridization events within the transmitter component. Input binding shifts the distribution to favor the input-bound conformation as a function of increasing input concentration and is translated to a change in the activity of the actuator, where a "ribozyme-active" state results in self-cleavage of the ribozyme (*21*).

Division of Chemistry and Chemical Engineering, California Institute of Technology, 1200 East California Boulevard, MC 210-41, Pasadena, CA 91125, USA.

*To whom correspondence should be addressed. E-mail: smolke@cheme.caltech.edu

Our results test the hypothesis that variation in gene expression is dictated by regulatory regions, extending recent studies of expression by quantitative trait-loci mapping and comparative expression studies that have been confined to closely related species (*26–30*). The apparent absence of overt trans influences could be explained by the modest amount of human DNA provided by a single copy of human chromosome 21 when compared with the complete mouse genome, as well as the absence of liver-specific transcriptional regulators on chromosome 21. The extent to which protein coding and cis-regulatory mutations contribute to changes in morphology, physiology, and behavior is actively debated in evolutionary biology (*3*, *12*, *13*). Myriad points of control influence gene expression; however, it has also been an unresolved question as to which of these mechanisms has the most influence globally. Here, we show that each layer of transcriptional regulation within the adult hepatocyte, from the binding of liver master regulators and chromatin remodeling complexes to the output of the transcriptional machinery, is directed primarily by DNA sequence. Although conservation of motifs alone cannot predict transcription factor binding, we show that within the genetic sequence there must be embedded adequate instructions to direct species-specific transcription.

References and Notes

1. E. H. Davidson, D. H. Erwin, *Science* **311**, 796 (2006).
2. K. S. Zaret, *Mech. Dev.* **92**, 83 (2000).
3. G. A. Wray, *Nat. Rev. Genet.* **8**, 206 (2007).
4. B. Li, M. Carey, J. L. Workman, *Cell* **128**, 707 (2007).
5. E. Guccione *et al.*, *Nat. Cell Biol.* **8**, 764 (2006).
6. L. Elnitski, V. X. Jin, P. J. Farnham, S. J. Jones, *Genome Res.* **16**, 1455 (2006).
7. D. T. Odom *et al.*, *Nat. Genet.* **39**, 730 (2007).
8. A. M. Moses *et al.*, *PLOS Comput. Biol.* **2**, e130 (2006).
9. A. R. Borneman *et al.*, *Science* **317**, 815 (2007).
10. E. Birney *et al.*, *Nature* **447**, 799 (2007).
11. B. E. Bernstein *et al.*, *Cell* **120**, 169 (2005).
12. H. E. Hoekstra, J. A. Coyne, *Evolution* **61**, 995 (2007).
13. S. B. Carroll, *Cell* **134**, 25 (2008).
14. A. O'Doherty *et al.*, *Science* **309**, 2033 (2005).
15. Materials and methods are available as supporting material on *Science* Online.
16. D. Kampa *et al.*, *Genome Res.* **14**, 331 (2004).
17. J. S. Carroll *et al.*, *Cell* **122**, 33 (2005).
18. S. Cereghini, *FASEB J.* **10**, 267 (1996).
19. J. Eeckhoute, B. Oxombre, P. Formstecher, P. Lefebvre, B. Laine, *Nucleic Acids Res.* **31**, 6640 (2003).
20. F. M. Sladek, M. D. Ruse Jr., L. Nepomuceno, S. M. Huang, M. R. Stallcup, *Mol. Cell. Biol.* **19**, 6509 (1999).
21. A. Rada-Iglesias *et al.*, *Hum. Mol. Genet.* **14**, 3435 (2005).
22. M. G. Guenther, S. S. Levine, L. A. Boyer, R. Jaenisch, R. A. Young, *Cell* **130**, 77 (2007).
23. M. Vermeulen *et al.*, *Cell* **131**, 58 (2007).
24. R. J. Sims 3rd *et al.*, *Mol. Cell* **28**, 665 (2007).
25. A. Barski *et al.*, *Cell* **129**, 823 (2007).
26. Y. Gilad, A. Oshlack, G. K. Smyth, T. P. Speed, K. P. White, *Nature* **440**, 242 (2006).
27. P. Khaitovich *et al.*, *Science* **309**, 1850 (2005).
28. P. J. Wittkopp, B. K. Haerum, A. G. Clark, *Nat. Genet.* **40**, 346 (2008).
29. C. C. Park *et al.*, *Nat. Genet.* **40**, 421 (2008).
30. Y. Gilad, S. A. Rifkin, J. K. Pritchard, *Trends Genet.* **24**, 408 (2008).

31. We are grateful to E. Jacobsen, R. Stark, I. Spiteri, B. Liu, J. Marioni, A. Lynch, J. Hadfield, N. Matthews, the Cambridge Research Institute (CRI) Genomics Core, CRI Bioinformatics Core, and Camgrid for technical assistance, and B. Gottgens and J. Ferrer for insightful advice. Supported by the European Research Council (D.T.O.); Royal Society Wolfson Research Merit Award (S.T.); Hutchison Whampoa (D.T.O., ST); Medical Research Council (E.F., VT); Wellcome Trust (E.F., V.T.); University of Cambridge (D.T.O., D.S., N.B.M., S.T.); and Cancer Research U.K. (D.T.O., M.D.W., N.B.M., S.T., D.S.). Data deposited under ArrayExpress accession numbers E-TABM-473 and E-TABM-474. M.D.W., N.B.M., D.S., D.T.O., and C.M.C. designed and performed experiments; N.B.M., M.D.W., and D.S. analyzed the data; L.V., V.T., M.D.W., and E.F. created, prepared, and provided Tc1 mouse tissues; and M.D.W., N.B.M., D.T.O., and S.T. wrote the manuscript. D.T.O. oversaw the work. The authors declare no competing interests.

Supporting Online Material

www.sciencemag.org/cgi/content/full/1160930/DC1
Materials and Methods
SOM Text
Figs. S1 to S12
Table S1

27 May 2008; accepted 3 September 2008
Published online 11 September 2008;
10.1126/science.1160930
Include this information when citing this paper.

Surface Sites for Engineering Allosteric Control in Proteins

Jeeyeon Lee,[1]* Madhusudan Natarajan,[2]* Vishal C. Nashine,[1] Michael Socolich,[2] Tina Vo,[2] William P. Russ,[2] Stephen J. Benkovic,[1] Rama Ranganathan[2]†

Statistical analyses of protein families reveal networks of coevolving amino acids that functionally link distantly positioned functional surfaces. Such linkages suggest a concept for engineering allosteric control into proteins: The intramolecular networks of two proteins could be joined across their surface sites such that the activity of one protein might control the activity of the other. We tested this idea by creating PAS-DHFR, a designed chimeric protein that connects a light-sensing signaling domain from a plant member of the Per/Arnt/Sim (PAS) family of proteins with *Escherichia coli* dihydrofolate reductase (DHFR). With no optimization, PAS-DHFR exhibited light-dependent catalytic activity that depended on the site of connection and on known signaling mechanisms in both proteins. PAS-DHFR serves as a proof of concept for engineering regulatory activities into proteins through interface design at conserved allosteric sites.

Proteins typically adopt well-packed three-dimensional structures in which amino acids are engaged in a dense network of contacts (*1*, *2*). This emphasizes the energetic importance of local interactions, but protein function also depends on nonlocal, long-range communication between amino acids. For example, information transmission between distant functional surfaces on signaling proteins (*3*), the distributed dynamics of amino acids involved in enzyme catalysis (*4–6*), and allosteric regulation in various proteins (*7*) all represent manifestations of nonlocal interactions between residues. To the extent that these features contribute to defining biological properties of protein lineages, we expect that the underlying mechanisms represent conserved rather than idiosyncratic features in protein families.

On the basis of this conjecture, methods such as statistical coupling analysis (SCA) quantitatively examine the long-term correlated evolution of amino acids in a protein family—the statistical signature of functional constraints arising from conserved communication between positions (*8*, *9*). This approach has identified sparse but physically connected networks of coevolving amino acids in the core of proteins (*8–12*). The connectivity of these networks is remarkable, given that a small fraction of total residues are involved and that no tertiary structural information is used in their identification. Empirical observation in several protein families shows that these networks connect the main functional site with distantly positioned secondary sites, enabling predictions of allosteric surfaces at which binding of regulatory molecules (or covalent modifications) might control protein function. Both literature studies and forward experimentation in specific model systems confirm these predictions (*8–12*). Thus, techniques such as SCA may provide a general tool for computational prediction of conserved allosteric surfaces.

The finding that certain surface sites might be statistical "hotspots" for functional interaction with active sites suggests an idea for engineering new regulatory mechanisms into proteins. What if two proteins were joined at surface sites such that their statistically correlated networks were juxtaposed and could form functional interactions (Fig. 1A)? If the connection sites are functionally linked to their respective active sites

[1]Department of Chemistry, Pennsylvania State University, University Park, PA 16802, USA. [2]Green Center for Systems Biology and Department of Pharmacology, University of Texas Southwestern Medical Center, Dallas, TX 75390, USA.

*These authors contributed equally to this work.
†To whom correspondence should be addressed. E-mail: rama.ranganathan@utsouthwestern.edu

crawl on FN along the blastocoel roof (*31*), and *fn1* controls migration of myocardial progenitors toward the midline (*26*, *32*)—a process that also requires another chemokine, *apelin* (*33*, *34*). However, gut defects have generally been interpreted as secondary to defects in mesoderm migration. In contrast, our studies reveal an earlier requirement for ECM-integrin interactions directly in endoderm migration.

We have shown that endoderm migration toward the anterior is genetically separable from other gastrulation movements (*35*). We propose that chemokine-dependent expression of integrin tethers the endoderm to the mesoderm, and that loss of this tether releases the endoderm to move anteriorly (Fig. 4); a secondary result is viscera bifida, because endodermal cells on either side [presumably containing organ progenitors (*8*)] have farther to converge dorsally and do not reach the midline in time to fuse. Viscera bifida–like syndromes in humans, including intestinal cysts and ectopic pancreatic or liver tissue, are relatively common and are not associated with spina bifida (ectoderm) (*36*), and defects in the CXCL12-CXCR4 signaling pathway may be an underlying cause.

For zebrafish endodermal cells, regulation of migration by controlling adhesion reconciles the recent observation that involuted endodermal cells initially move via a "random walk" rather than the directed migration displayed by the mesoderm (*37*). Classically, chemokines are cytokines that induce chemotaxis in responding cells; CXCL12-CXCR4 interactions control homing of hematopoietic stem cells to the bone marrow, as well as migration of germ cells, neuronal progenitors, and several metastatic cancers (*15*–*18*, *27*). In some of these cases, however, there is evidence for a system more like the tether described here, where receptor-expressing cells are confined to a territory defined by ligand-expressing cells. Thus, chemokine-dependent changes in adhesion to the ECM may influence cell migration rates and directionality in many developmental and disease contexts.

References and Notes

1. L. Solnica-Krezel, *Curr. Biol.* **15**, R213 (2005).
2. D. J. Roberts, *Dev. Dyn.* **219**, 109 (2000).
3. J. Alexander *et al.*, *Dev. Biol.* **215**, 343 (1999).
4. F. Biemar *et al.*, *Dev. Biol.* **230**, 189 (2001).
5. E. A. Ober *et al.*, *Nature* **442**, 688 (2006).
6. R. Keller, *Science* **298**, 1950 (2002).
7. A. F. Schier, *Annu. Rev. Cell Dev. Biol.* **19**, 589 (2003).
8. R. M. Warga, C. Nusslein-Volhard, *Development* **126**, 827 (1999).
9. S. W. Chong *et al.*, *Mech. Dev.* **109**, 347 (2001).
10. K. Dickinson *et al.*, *Dev. Dyn.* **235**, 368 (2006).
11. A. Fukui *et al.*, *Biochem. Biophys. Res. Commun.* **354**, 472 (2007).
12. K. E. McGrath *et al.*, *Dev. Biol.* **213**, 442 (1999).
13. F. Yusuf *et al.*, *Anat. Embryol.* **210**, 35 (2005).
14. K. Tachibana *et al.*, *Nature* **393**, 591 (1998).
15. N. B. David *et al.*, *Proc. Natl. Acad. Sci. U.S.A.* **99**, 16297 (2002).
16. H. Knaut *et al.*, *Neuron* **47**, 653 (2005).
17. Q. Li *et al.*, *J. Neurosci.* **25**, 1711 (2005).
18. E. Raz, *Curr. Opin. Cell Biol.* **16**, 169 (2004).
19. H. A. Field *et al.*, *Dev. Biol.* **253**, 279 (2003).
20. T. N. Hartmann *et al.*, *Oncogene* **24**, 4462 (2005).
21. J. E. Howard *et al.*, *Mech. Dev.* **38**, 109 (1992).
22. J. Jones *et al.*, *Exp. Cell Res.* **313**, 4051 (2007).
23. F. M. Watt, K. J. Hodivala, *Curr. Biol.* **4**, 270 (1994).
24. R. Winklbauer, R. E. Keller, *Dev. Biol.* **177**, 413 (1996).
25. A. J. Pelletier *et al.*, *Blood* **96**, 2682 (2000).
26. L. A. Trinh, D. Y. Stainier, *Dev. Cell* **6**, 371 (2004).
27. J. Juarez, L. Bendall, *Histol. Histopathol.* **19**, 299 (2004).
28. E. Ruoslahti, *Annu. Rev. Cell Dev. Biol.* **12**, 697 (1996).
29. A. P. Mould *et al.*, *BMC Cell Biol.* **7**, 24 (2006).
30. J. A. Montero *et al.*, *Development* **132**, 1187 (2005).
31. R. Winklbauer *et al.*, *Int. J. Dev. Biol.* **40**, 305 (1996).
32. T. Sakaguchi *et al.*, *Development* **133**, 4063 (2006).
33. I. C. Scott *et al.*, *Dev. Cell* **12**, 403 (2007).
34. X. X. Zeng *et al.*, *Dev. Cell* **12**, 391 (2007).
35. R. Keller *et al.*, *Differentiation* **71**, 171 (2003).
36. R. E. Stevenson *et al.*, *Human Malformations and Related Anomalies* (Oxford Univ. Press, New York, 1993).
37. G. Pezeron *et al.*, *Curr. Biol.* **18**, 276 (2008).

38. We thank E. Raz for *cxcl12b* and *cxcr4a* constructs; our laboratory colleagues, especially S. Piloto for help with qPCR and T. Hoffman for help with itgb1b constructs; and I. Blitz for reviewing the manuscript. Supported by NIH grants R01NS41353 and R01DE13828.

Supporting Online Material

www.sciencemag.org/cgi/content/full/1160038/DC1
Materials and Methods
Figs. S1 to S7
Table S1
References

5 May 2008; accepted 13 August 2008
Published online 21 August 2008;
10.1126/science.1160038
Include this information when citing this paper.

Molecular Architecture of the "Stressosome," a Signal Integration and Transduction Hub

Jon Marles-Wright,[1]* Tim Grant,[2]* Olivier Delumeau,[1]† Gijs van Duinen,[2]‡ Susan J. Firbank,[1] Peter J. Lewis,[3] James W. Murray,[1]§ Joseph A. Newman,[1] Maureen B. Quin,[1] Paul R. Race,[1] Alexis Rohou,[2] Willem Tichelaar,[2]‖ Marin van Heel,[2]¶ Richard J. Lewis[1]¶

A commonly used strategy by microorganisms to survive multiple stresses involves a signal transduction cascade that increases the expression of stress-responsive genes. Stress signals can be integrated by a multiprotein signaling hub that responds to various signals to effect a single outcome. We obtained a medium-resolution cryo–electron microscopy reconstruction of the 1.8-megadalton "stressosome" from *Bacillus subtilis*. Fitting known crystal structures of components into this reconstruction gave a pseudoatomic structure, which had a virus capsid–like core with sensory extensions. We suggest that the different sensory extensions respond to different signals, whereas the conserved domains in the core integrate the varied signals. The architecture of the stressosome provides the potential for cooperativity, suggesting that the response could be tuned dependent on the magnitude of chemophysical insult.

Microorganisms experiencing a fluctuating environment commonly exhibit a short-lived, reversible response that allows survival and recovery of the cell (*1*). In Gram-positive bacteria such as *Bacillus subtilis*, one such signaling cascade ultimately leads to the activation of the general stress sigma factor, σ^B (fig. S1), and enhanced transcription of its large regulon to provide a global response to the imposed stress (*2*, *3*). The stressosome is the signaling hub that integrates multiple physical stress signals (*4*–*7*) and orchestrates a single signaling outcome: the activation of σ^B. The stressosome is found in many microbial phyla, including representatives of the Methanomicrobiales branch of the Euryarchaea and, within Bacteria, the Proteobacteria, the Firmicutes, the Actinobacteria, the Cyanobacteria, and the *Bacteroides* and *Deinococcus* groups (*8*). The downstream chromosomal organization in these organisms points to the involvement of stressosome orthologs in regulating aerotaxis, a variety of two-component signaling systems, and the biosynthesis of secondary messenger signaling molecules. Thus, the stressosome appears to have evolved to provide a common solution to the problem of signal integration.

In *Bacillus*, the stressosome is a ~1.8 MD supramolecular complex comprising multiple copies of the regulator of sigma B proteins: RsbS, RsbR, and four paralogs of RsbR (*7*, *9*–*13*). The C-terminal domain of RsbR and its paralogs is conserved and is similar in sequence to RsbS. By contrast, the N-terminal domains of the RsbR paralogs show high sequence variability, suggesting that they function as sensors, whereas the C-terminal domains integrate the various signals. A third protein, RsbT, interacts with RsbR:RsbS complexes (*9*) to transmit integrated environmental signals into the σ^B activation pathway. The ability of stressosomes to integrate multiple inputs to effect a single output represents a departure from the more common one- and two-component signaling systems in prokaryotes (*14*). These systems typically convert a single signal into a single outcome, usually the transcriptional modulation of small regulons in response to specific metabolic changes (*15*). The activity of the stressosome can be reconstituted both in vitro and in vivo by complexes consisting